

Supplementary information

**Fluorescent dyes and probes for super-resolution microscopy of
microtubules and tracheoles in living cells and tissues**

Gražvydas Lukinavičius*, Gyuzel Y. Mitronova, Sebastian Schnorrenberg, Alexey N. Butkevich,
Hannah Barthel, Vladimir N. Belov and Stefan W. Hell

Max Planck Institute for Biophysical Chemistry, Department of NanoBiophotonics, Am Fassberg 11, 37077
Göttingen, Germany

*Corresponding author's e-mail: grazvydas.lukinavicius@mpibpc.mpg.de.

Supplementary inventory

Supplementary inventory	2
Supplementary Figures and Videos	3
Figure S1. Microtubule-paclitaxel complex model	3
Figure S2. Determination of $D_{0.5}$ for 510R dye	4
Figure S3. Spectral properties of the tubulin probes	5
Figure S4. Aggregation of the tubulin probes	6
Figure S5. Quantification of the tubulin probes aggregation	7
Figure S6. Fluorescence increase of the tubulin probes upon binding to polymerized tubulin	8
Figure S7. Tubulin stabilization is induced by the fluorescent probes	9
Figure S8. Cell cycle perturbation induced by fluorescent tubulin probes	10
Figure S9. Absence of correlation between apparent tubulin polymerization rate and cytotoxicity	11
Figure S10. Confocal images of living human fibroblasts stained with the fluorescent tubulin probes	12
Figure S11. Confocal images of living fibroblasts stained with different concentrations of the fluorescent tubulin probes	13
Figure S12. Confocal and STED (775 nm) images of living human fibroblasts or <i>Drosophila melanogaster</i> larvae living muscle tissue stained with the tubulin probes	14
Figure S13. Confocal and STED (775 nm) images of living human fibroblasts stained with the sub-cytotoxic concentrations of tubulin probes	15
Figure S14. STED (775 nm) image of <i>Drosophila melanogaster</i> larvae living muscle tissue showing microtubule and tracheole staining	16
Figure S15. Tracheole-specific staining	17
Figure S16. Confocal images of <i>Drosophila melanogaster</i> larvae tracheoles and cuticle	18
Video S1. Confocal time series of microtubule dynamics in living human primary dermal fibroblasts stained with 62.5 nM 510R-CTX probe	19
Video S2. Confocal time series of microtubule dynamics in living human primary dermal fibroblasts stained with 62.5 nM 580CP-LTX probe	19
Video S3. Confocal time series of microtubule dynamics in living human primary dermal fibroblasts stained with 250 nM GeR-DTX probe	19
Video S4. Confocal time series of microtubule dynamics in living human primary dermal fibroblasts stained with 62.5 nM SiR-CTX probe	19
Video S5. Confocal time series of microtubule dynamics in <i>Drosophila melanogaster</i> larvae living muscle tissue stained with 1 μ M SiR-CTX probe	19
Supplementary Tables	20
Table S1. Photophysical properties of fluorescent dyes used in this study	20
Table S2. Photophysical properties of fluorescent tubulin probes	20
Table S3. Properties of fluorescent tubulin probes	20
Supplementary methods	21
General materials and methods	21
Chemical synthesis	21
510R-C8-COOH	21
510R-DTX	22
510R-CTX	23
510R-LTX	24
580CP-CTX	24
580CP-LTX	25
SiR-CTX	25
SiR-LTX	26
GeR-CTX	27
GeR-LTX	28

Supplementary Figures and Videos

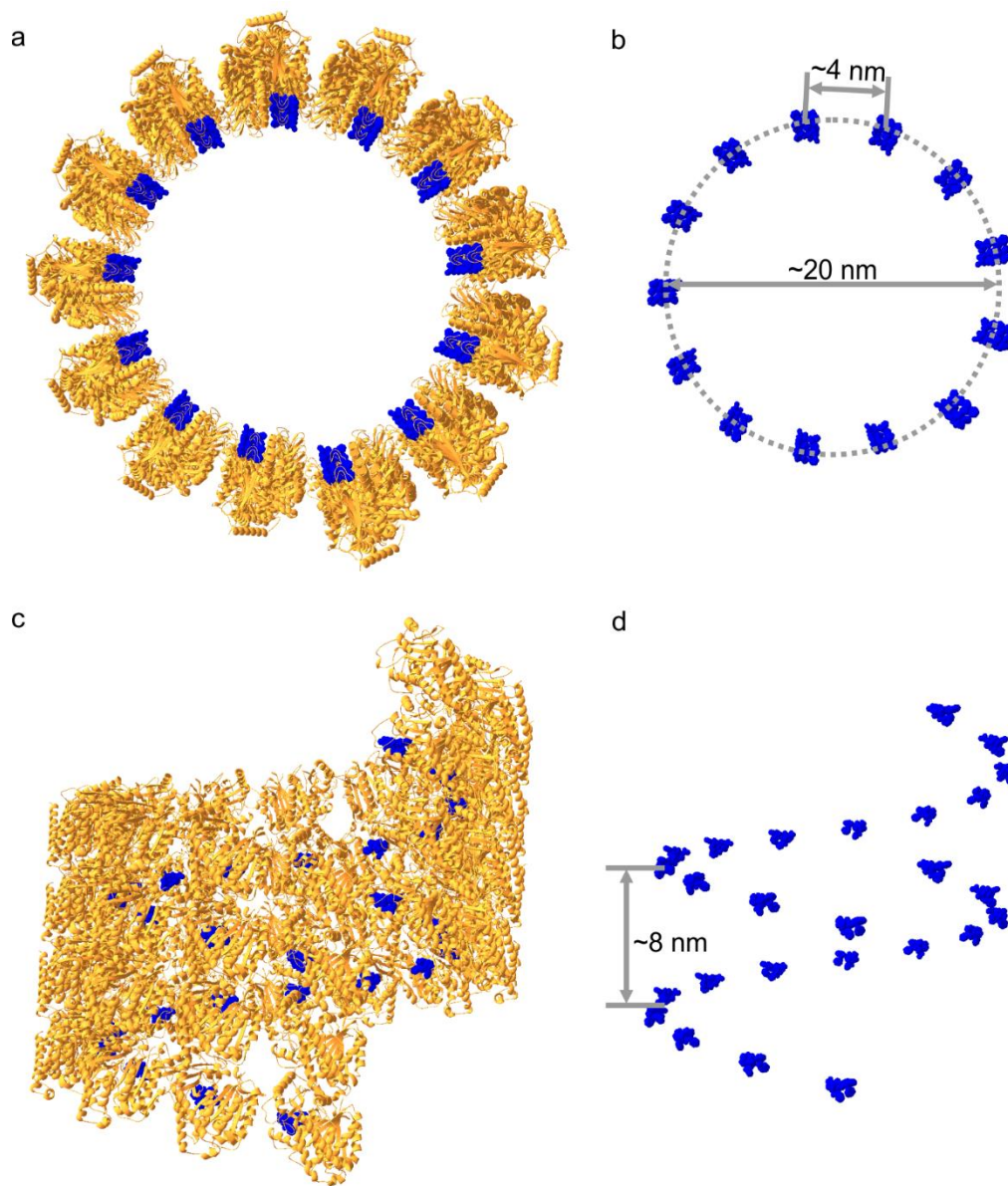


Figure S1. Microtubule-paclitaxel complex model. (a) Top view of microtubule composed of tubulin dimers bound to paclitaxel. (b) Same view as in (a), but protein molecules are omitted. (c) Side view of microtubule composed of tubulin dimers bound to paclitaxel. (d) Same view as in (c), but protein molecules are omitted. Distances between paclitaxel binding sites in the cryo-electron microscopy model of the microtubule. Protein is presented as yellow ribbons, paclitaxel – space-filling model. GTP, GDP and Mg^{2+} molecules are omitted for clarity. PDB ID: 5SYF¹.

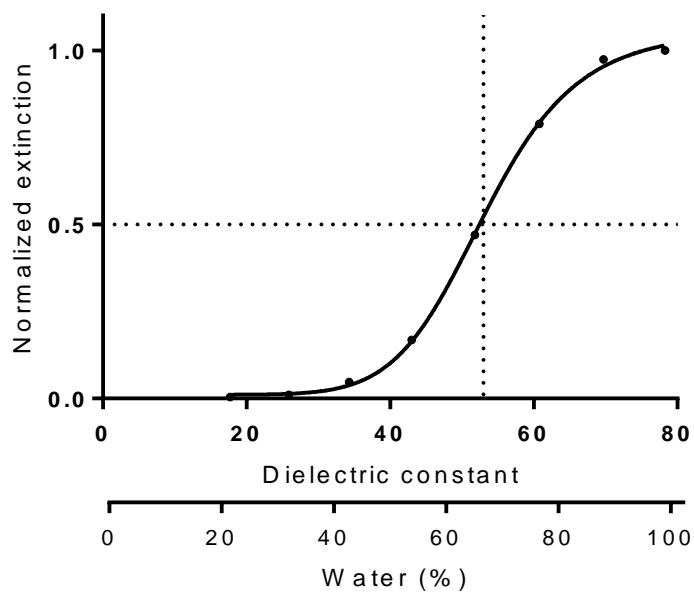


Figure S2. Determination of $D_{0.5}$ for 510R dye. Normalized extinction ϵ/ϵ_{\max} at λ_{\max} of 510R dye versus dielectric constant D of dioxane-water mixtures². The $D_{0.5}$ value of the dye corresponds to the intersection of the interpolated graph with $\epsilon/\epsilon_{\max} = 0.5$ line.

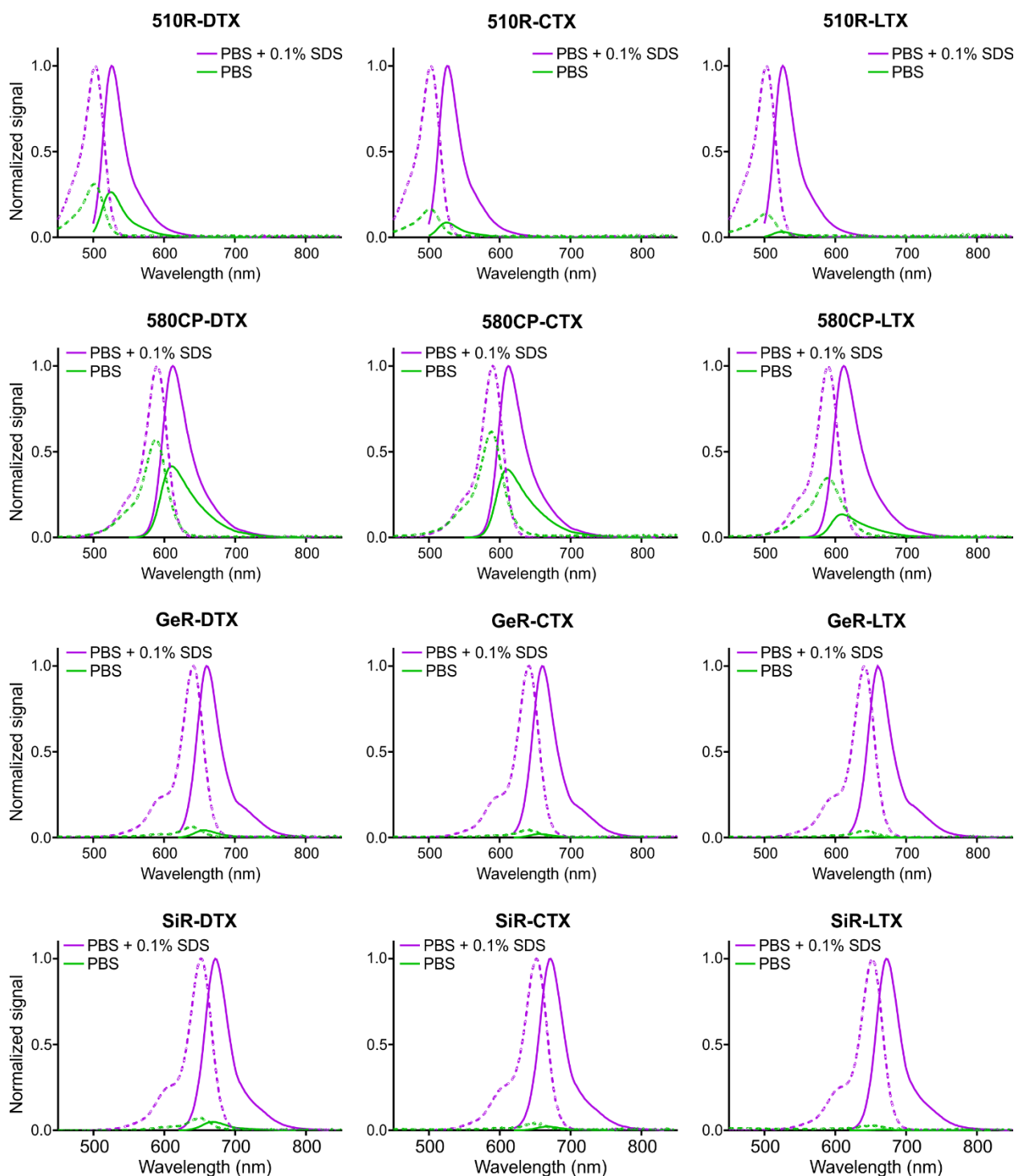


Figure S3. Spectral properties of the tubulin probes. Absorbance (dotted line) and fluorescence (solid line) spectra of tubulin probes in PBS (green) and PBS containing 0.1% SDS (magenta). 2 μM probes were incubated at room temperature for 1 h before measurements. Spectra are normalized to the samples containing 0.1% SDS and presented as averages of three independent experiments.

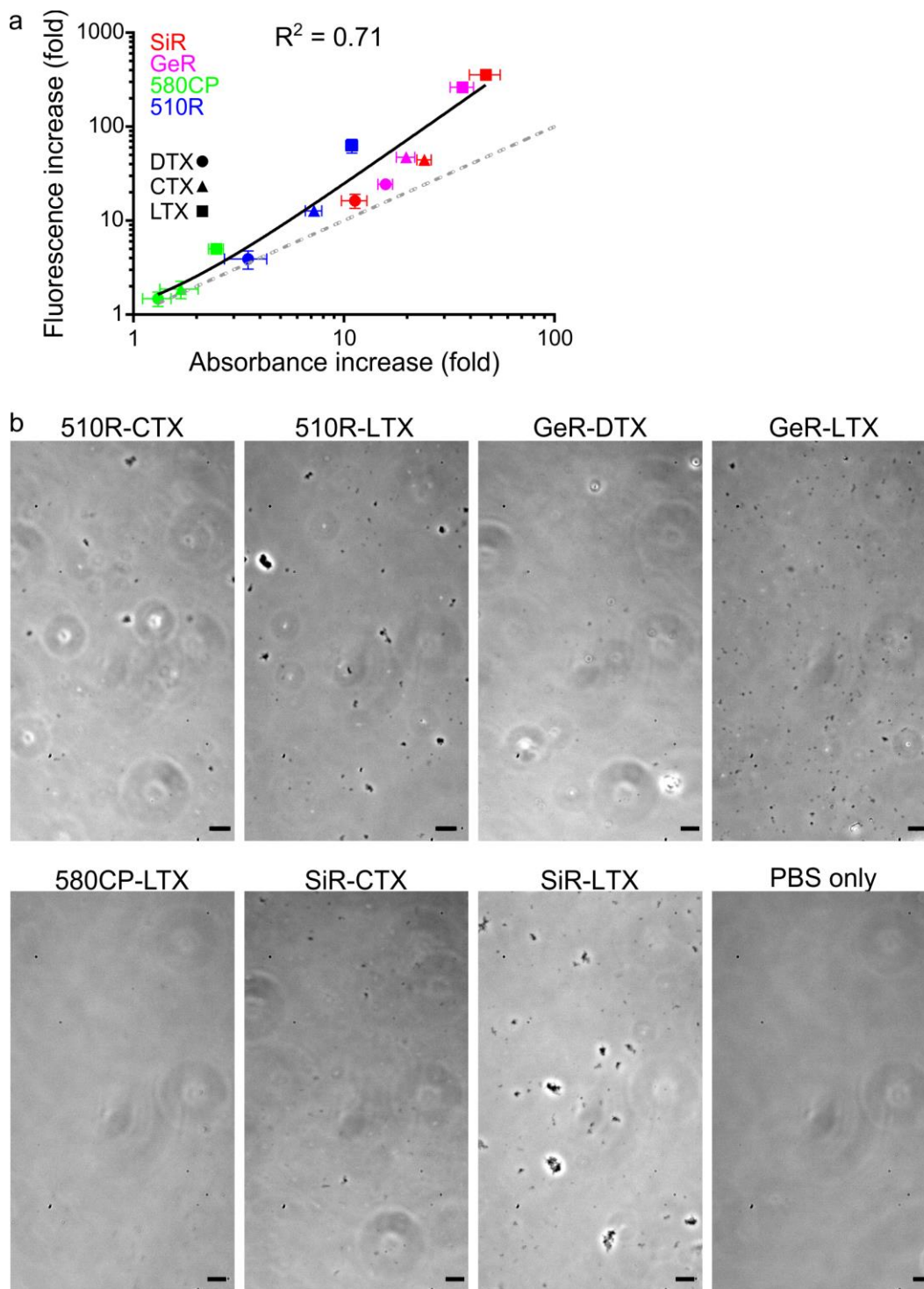
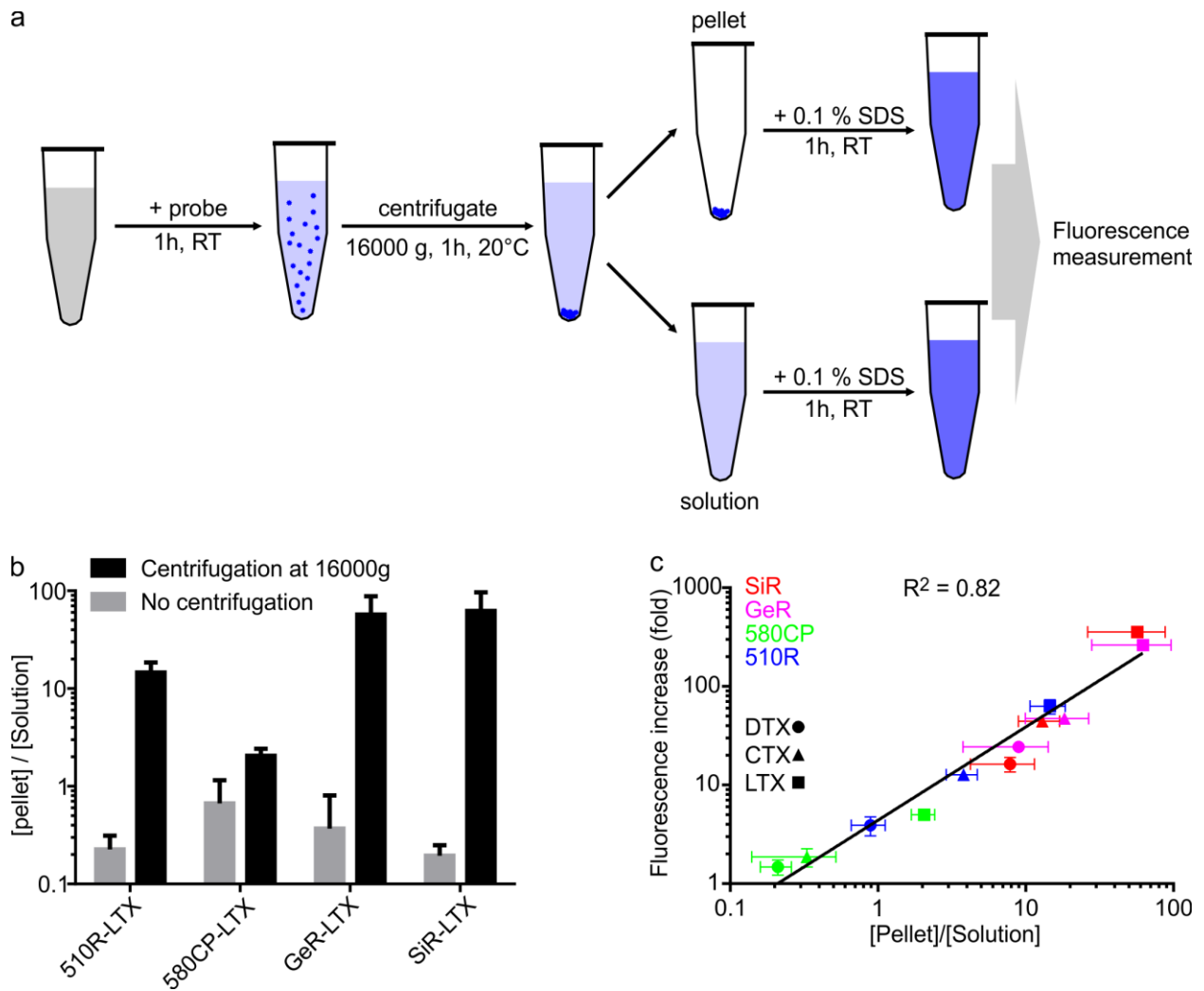


Figure S4. Aggregation of the tubulin probes. (a) Correlation between absorbance and fluorescence increases in PBS upon 0.1% SDS addition. Solid grey line shows data points fitting with correlation coefficient equal to 0.71 and dotted grey line corresponds to $y = x$ equation. Blue dots correspond to 510R derivatives, green dots – 580CP derivatives, purple dots – GeR derivatives and red dots – SiR derivatives. (b) Phase contrast light microscopy images of 2 μM probes incubated for 1 h at room temperature in PBS. Images taken on Motic AE2000 inverted microscope equipped with 20x/0.3 air objective and camera DMK 72BUC02 (Imaging Source). Scale bar 10 μm .



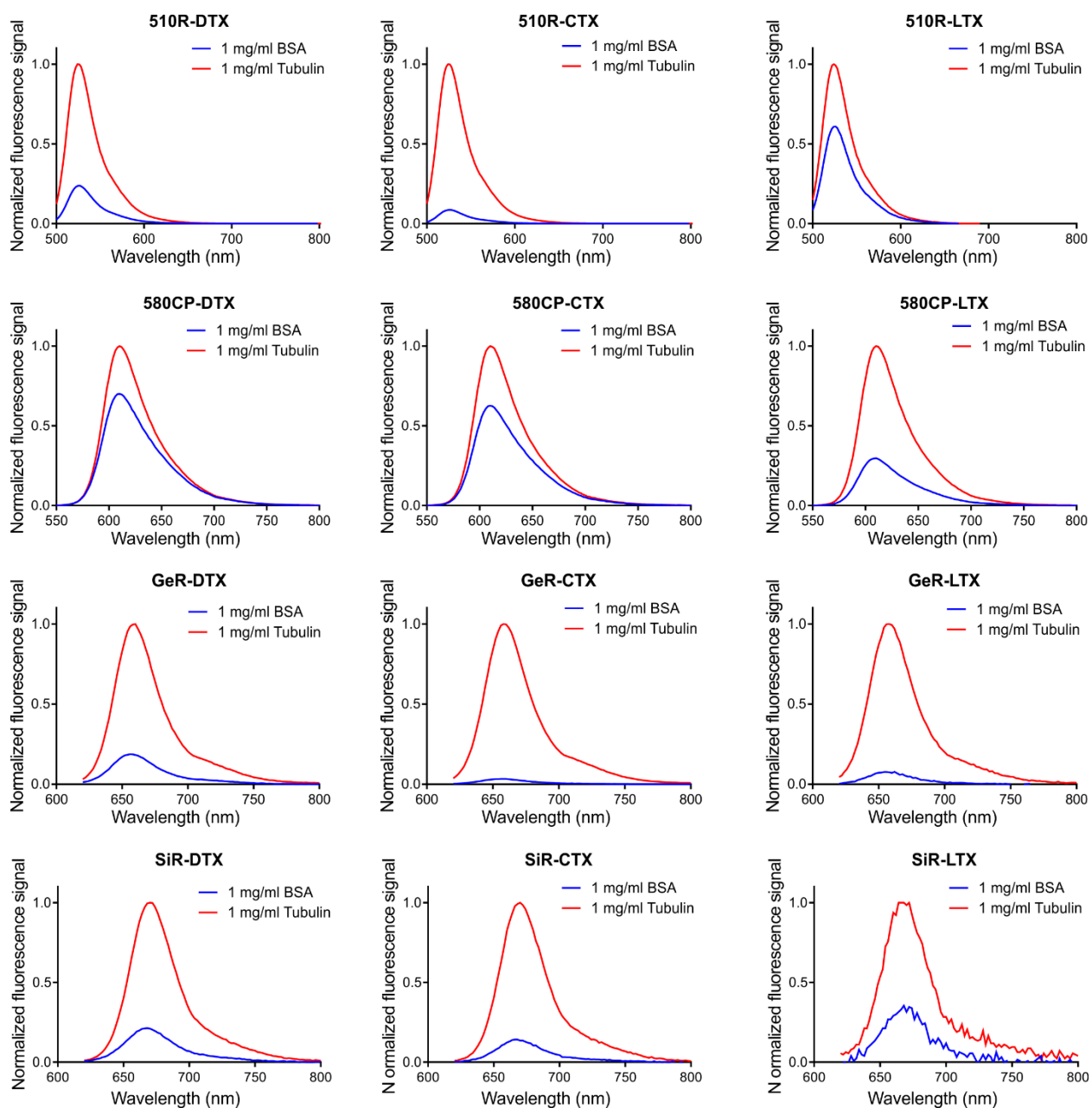


Figure S6. Fluorescence increase of the tubulin probes upon binding to polymerized tubulin. Spectra were recorded after incubating of 2 μ M probes with 1 mg/ml BSA (blue) or tubulin (red) at 37 $^{\circ}$ C for 5 h to ensure complete tubulin polymerization. Spectra are presented as averages of three independently repeated experiments (N=3).

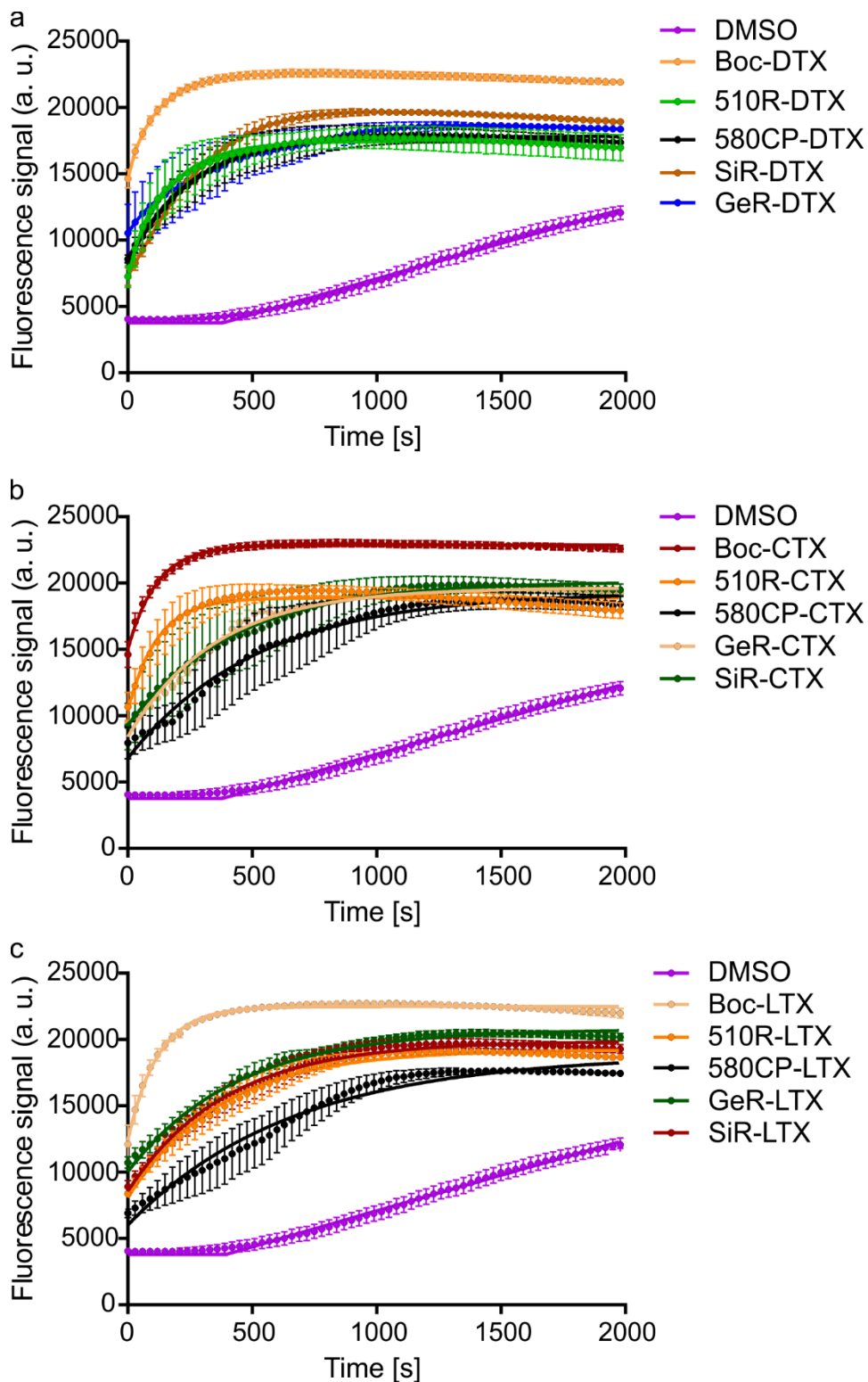


Figure S7. Tubulin stabilization is induced by the fluorescent probes. Tubulin stabilization induced by 3 μ M tubulin probes or their precursors results in increased apparent polymerization rate at 37 $^{\circ}$ C. The following stabilizing reagents were tested: **(a)** docetaxel or its derivatives, **(b)** cabazitaxel or its derivatives, or **(c)** larotaxel or its derivatives. Experimental data are averages of three independently repeated experiments (N=3) and presented as means with standard error of the mean.

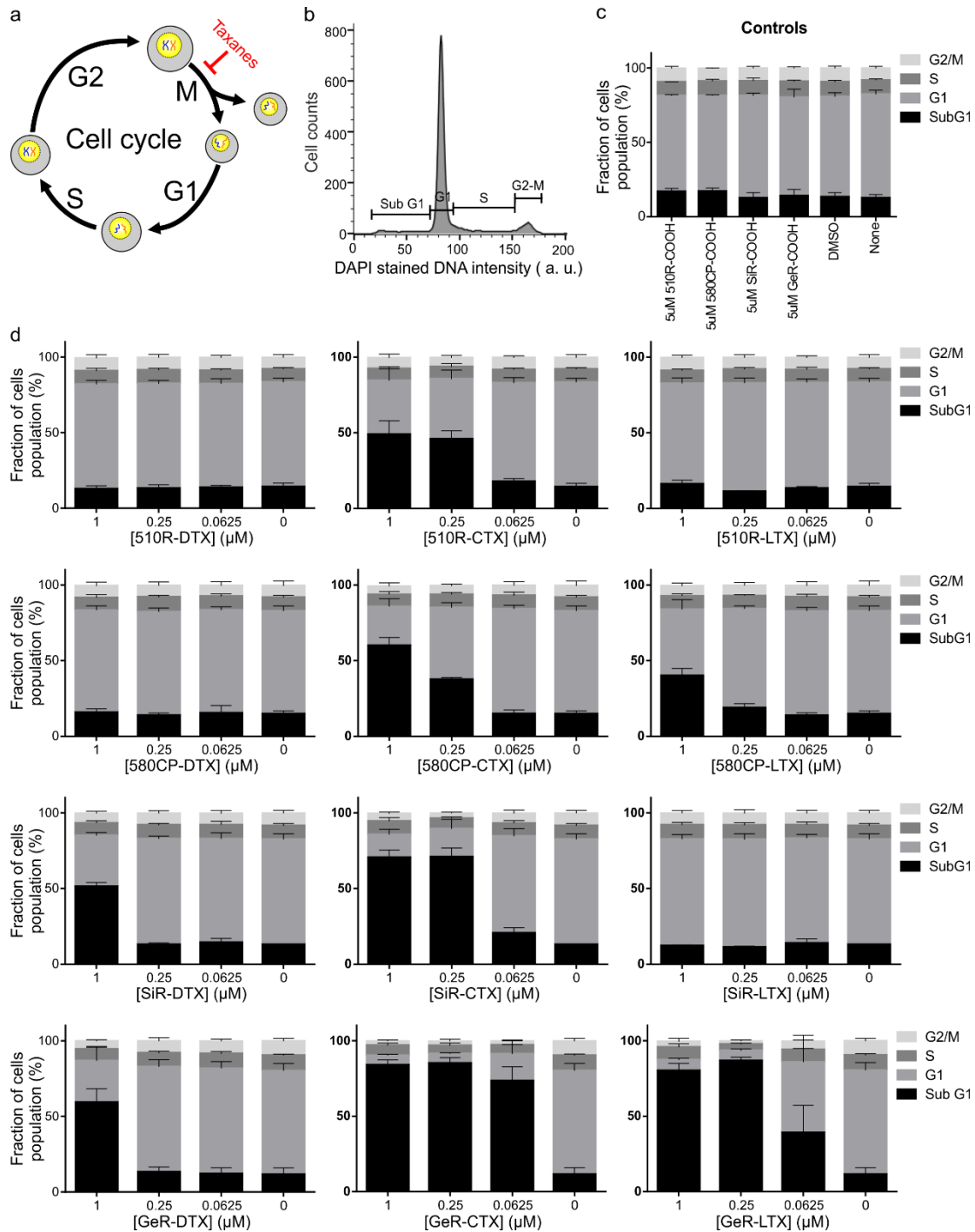


Figure S8. Cell cycle perturbation induced by fluorescent tubulin probes. (a) Cytotoxicity of taxanes results from the inhibition of the cell cycle at the stage of mitosis (M) phase. (b) A representative histogram of DNA content distribution in HeLa cell populations treated with DMSO only. Indicated cell cycle phases (Sub G1, G1, S and G2-M) are identified by the amount of DNA in the measured cells. (c) Outcome of control experiments when cells were untreated or treated with high concentrations of free carboxylic acid dyes or DMSO only. (d) Cytotoxicity measurements of tubulin probes. HeLa cells were incubated with variable concentrations of the tubulin probes at 37 °C for 24 h in a humidified 5% CO₂ incubator. Experimental data are averages of the three independent experiments (N=3) and presented as means with standard deviations. Cytometry sample size n = 10000 cells.

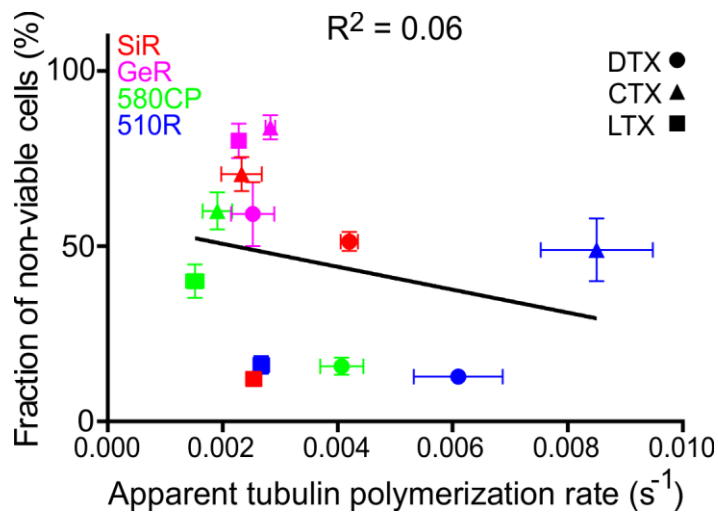


Figure S9. Absence of correlation between apparent tubulin polymerization rate and cytotoxicity. Fraction of non-viable cells corresponds to the cells containing DNA amount corresponding to sub G1 phase. Before the measurement, Hela cells were incubated with 1 μM probes for 24 h in a humidified incubator at 37 °C and 5% CO₂. Tubulin polymerization rate estimated using Cytoskeleton tubulin polymerization kit (cat. BK011P) and 3 μM probes. Experimental data are averages of the three independent experiments (N=3) and presented as means with standard deviations.

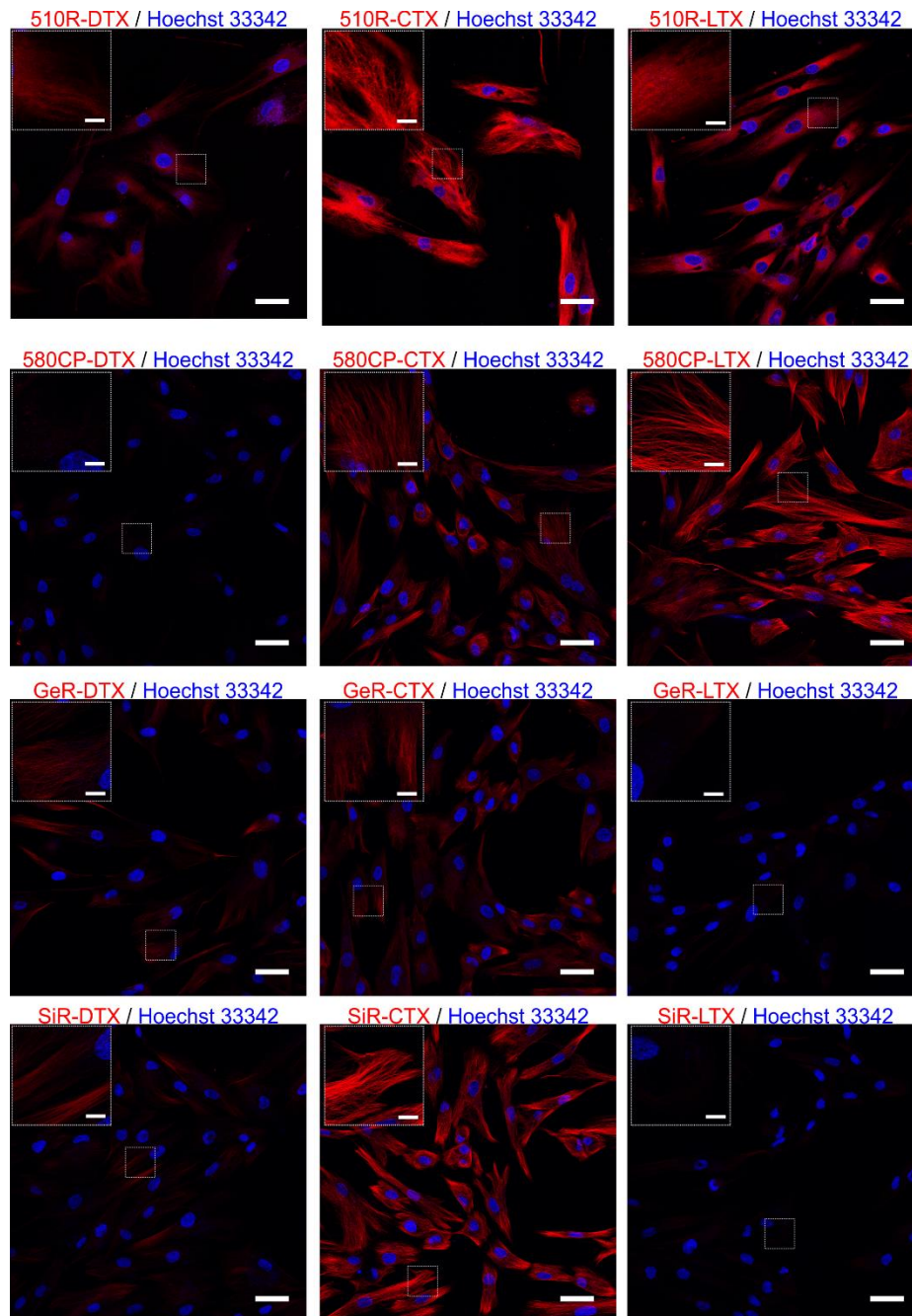


Figure S10. Confocal images of living human fibroblasts stained with the fluorescent tubulin probes. Living human fibroblasts were stained with a mixture of 1 μM probe and 0.1 $\mu\text{g/ml}$ Hoechst 33342 in DMEM growth medium containing 10% FBS. The cells were incubated at 37 $^{\circ}\text{C}$ for 1 h and washed two times with HBSS and imaged on Leica SP8 confocal microscope using the same excitation powers for the three respective dye conjugates (-DTX, -CTX and -LTX) in the DMEM growth medium containing 10% FBS. Inserts show images of zoom-in areas at the positions indicated by white rectangles in the large fields of view. Images of the respective dye conjugates (-DTX, -CTX and -LTX) are depicted using the same lookup table. Scale bars: 50 μm in the large fields of view and 10 μm in the inserts.

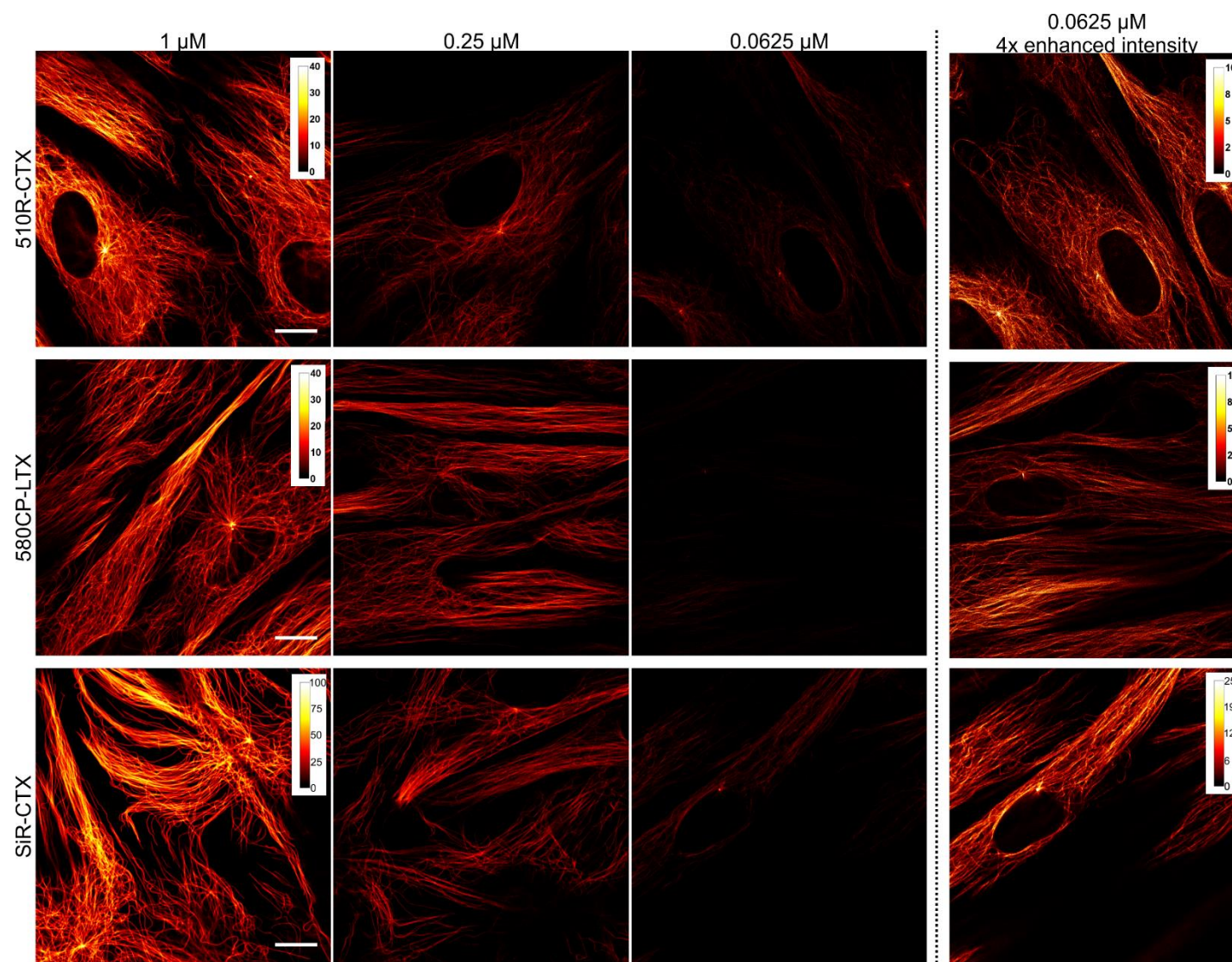


Figure S11. Confocal images of living fibroblasts stained with different concentrations of the fluorescent tubulin probes. Living human fibroblasts were incubated with the indicated concentration of the tubulin probes in growth medium containing 10% FBS at 37 °C for 1 h, washed two times with HBSS and imaged on an Abberior STED 775 QUAD scanning microscope in DMEM growth medium. Scale bars: 10 μm.

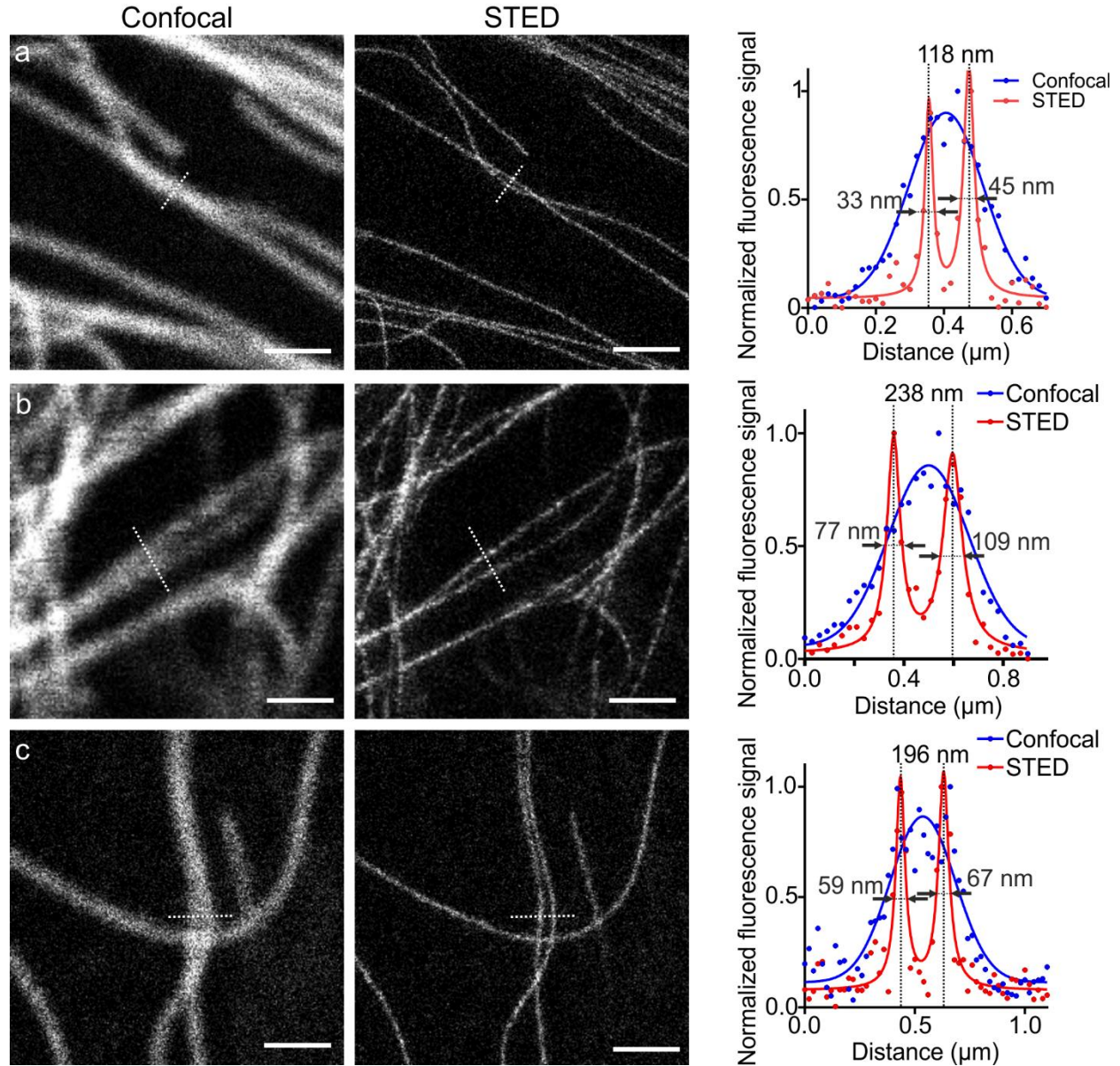


Figure S12. Confocal and STED (775 nm) images of living human fibroblasts or *Drosophila melanogaster* larvae living muscle tissue stained with the tubulin probes. (a) Image of living human fibroblasts stained with 2 μM SiR-CTX. (b) Image of the muscle tissue stained with 2 μM 580CP-LTX. (c) Image of the muscle tissue stained with 4 μM SiR-CTX. Intensity profiles shown on the right are taken at the positions indicated in the corresponding images on the left by the dotted lines. Living human fibroblasts were incubated with the indicated concentration of the tubulin probes in growth medium containing 10% FBS at 37 $^{\circ}\text{C}$ for 1 h, washed two times with HBSS and imaged. *D. melanogaster* larvae muscle tissue was incubated with indicated probes or mixtures for 1 h at room temperature and washed once with PBS before imaging. The distances between Lorentz distribution maxima are indicated above the peaks. Images were acquired on an Abberior STED 775 QUAD scanning microscope. The numbers next to arrows indicate full widths at half maximum (FWHM) of fitted dual Lorentz distributions. Confocal profiles (blue) and STED profiles (red) are fitted to Gaussian and Lorentz distributions, respectively. Scale bars: 1 μm .

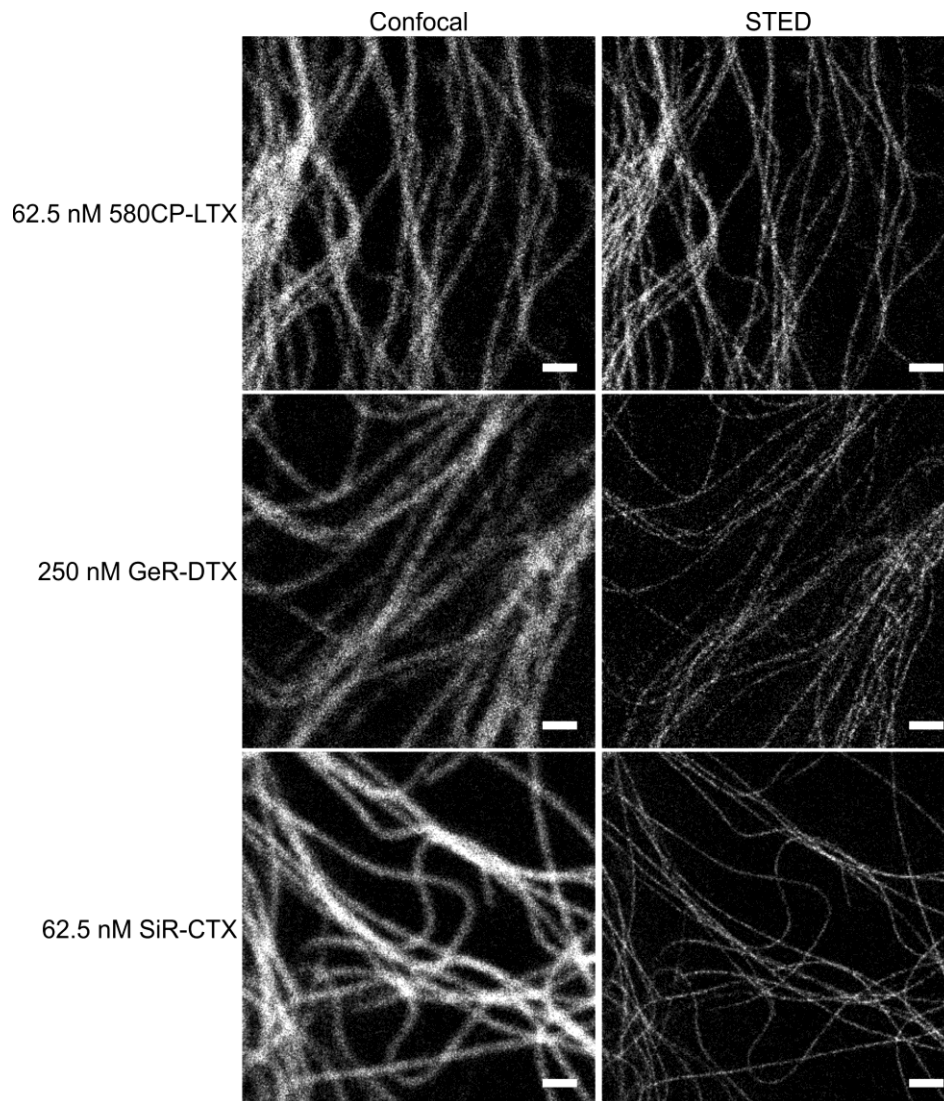


Figure S13. Confocal and STED (775 nm) images of living human fibroblasts stained with the sub-cytotoxic concentrations of tubulin probes. Living human fibroblasts were incubated with the indicated concentration of the tubulin probes in growth medium containing 10% FBS at 37 °C for 1 h, washed two times with HBSS and imaged. . Images were acquired on an Abberior STED 775 QUAD scanning microscope. Scale bars: 1 μ m.

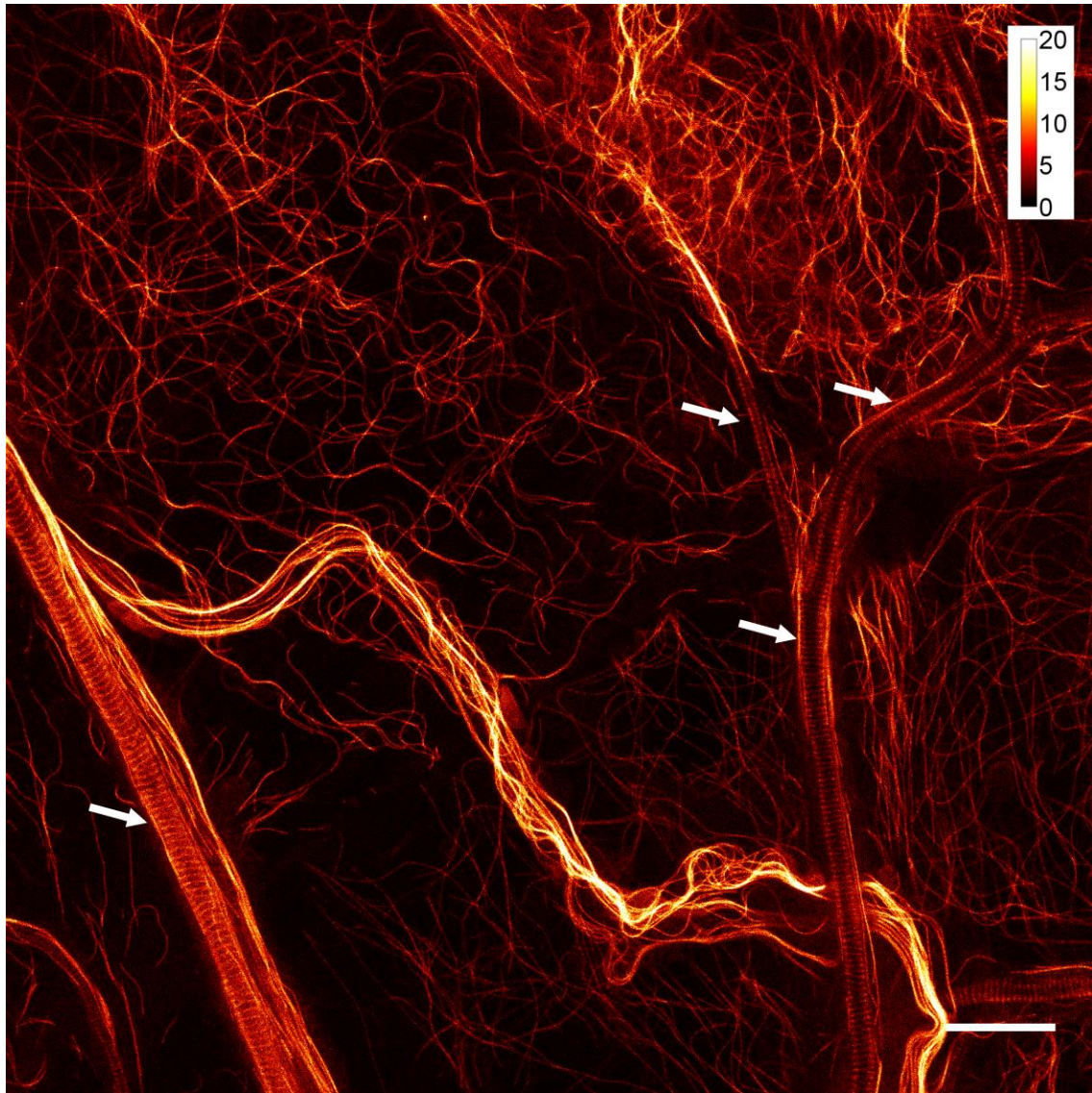


Figure S14. STED (775 nm) image of *Drosophila melanogaster* larvae living muscle tissue showing microtubule and tracheole staining. White arrows indicate stained taenidia in the tracheoles. Larvae muscle tissue was incubated with 2 μ M 580CP-LTX probe in PBS for 1 h at room temperature and washed once with PBS before imaging. Image was acquired on an Abberior STED 775 QUAD scanning microscope. Scale bars: 5 μ m.

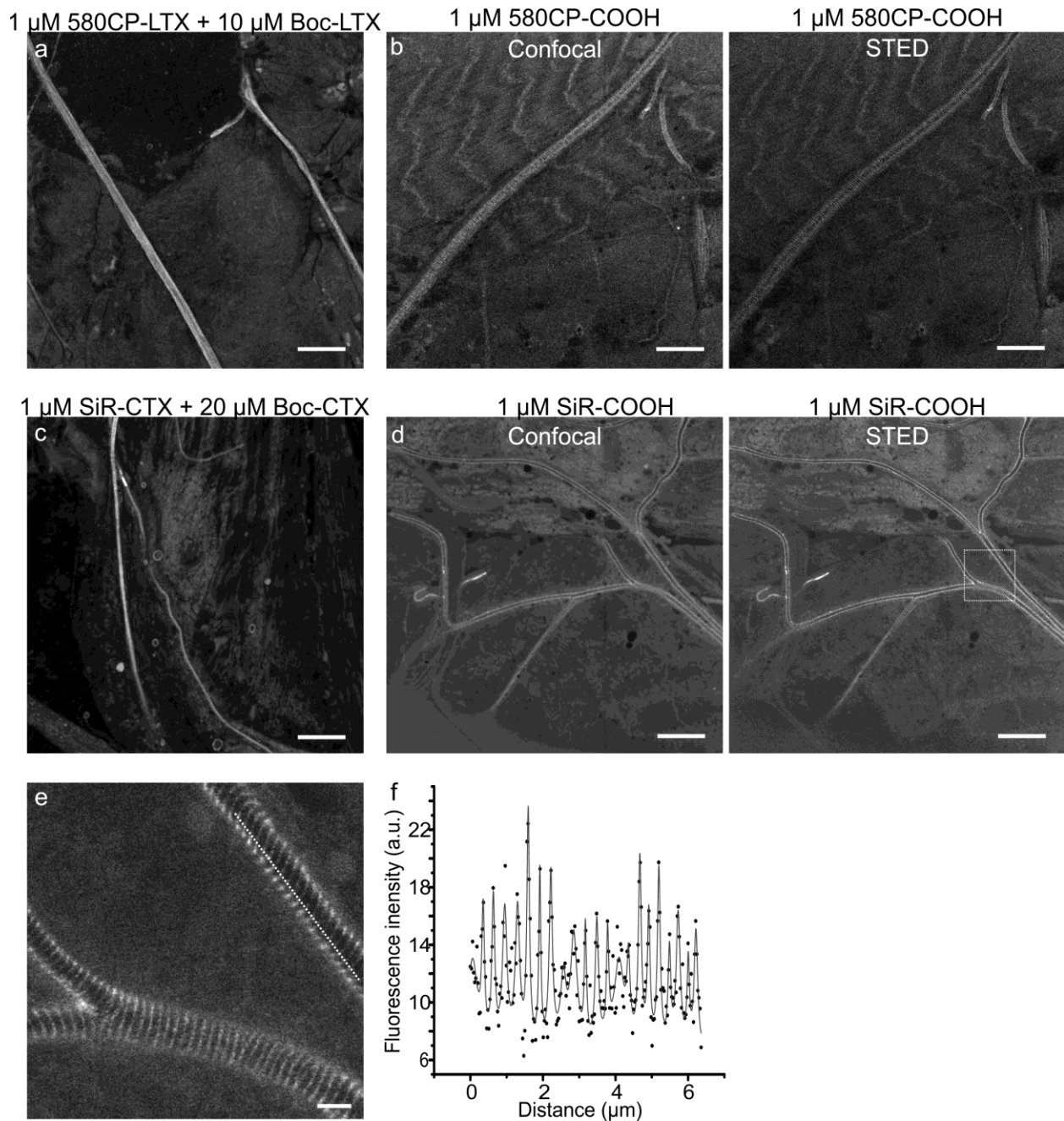


Figure S15. Tracheole-specific staining. (a) Confocal image of tracheoles stained with a mixture of 1 μM 580CP-CTX and 10 μM non-fluorescent Boc-LTX. (b) Confocal and STED images of tracheoles stained with 1 μM 580CP-COOH. (c) Confocal image of tracheoles stained with a mix of 1 μM SiR-CTX and 20 μM non-fluorescent Boc-CTX. (d) Confocal and STED images of tracheoles stained with 1 μM SiR-COOH. (e) Zoom-in area indicated by white rectangle in STED image in panel (d). Scale bar: 1 μm . (f) Line profile of fluorescence intensity measured along the dotted line depicted in (e). *Drosophila melanogaster* larvae muscle tissue was incubated with indicated probes or mixtures for 1 h at room temperature and washed once with PBS before imaging. Images were acquired on an Abberior STED 775 QUAD scanning microscope. Scale bar: 10 μm .

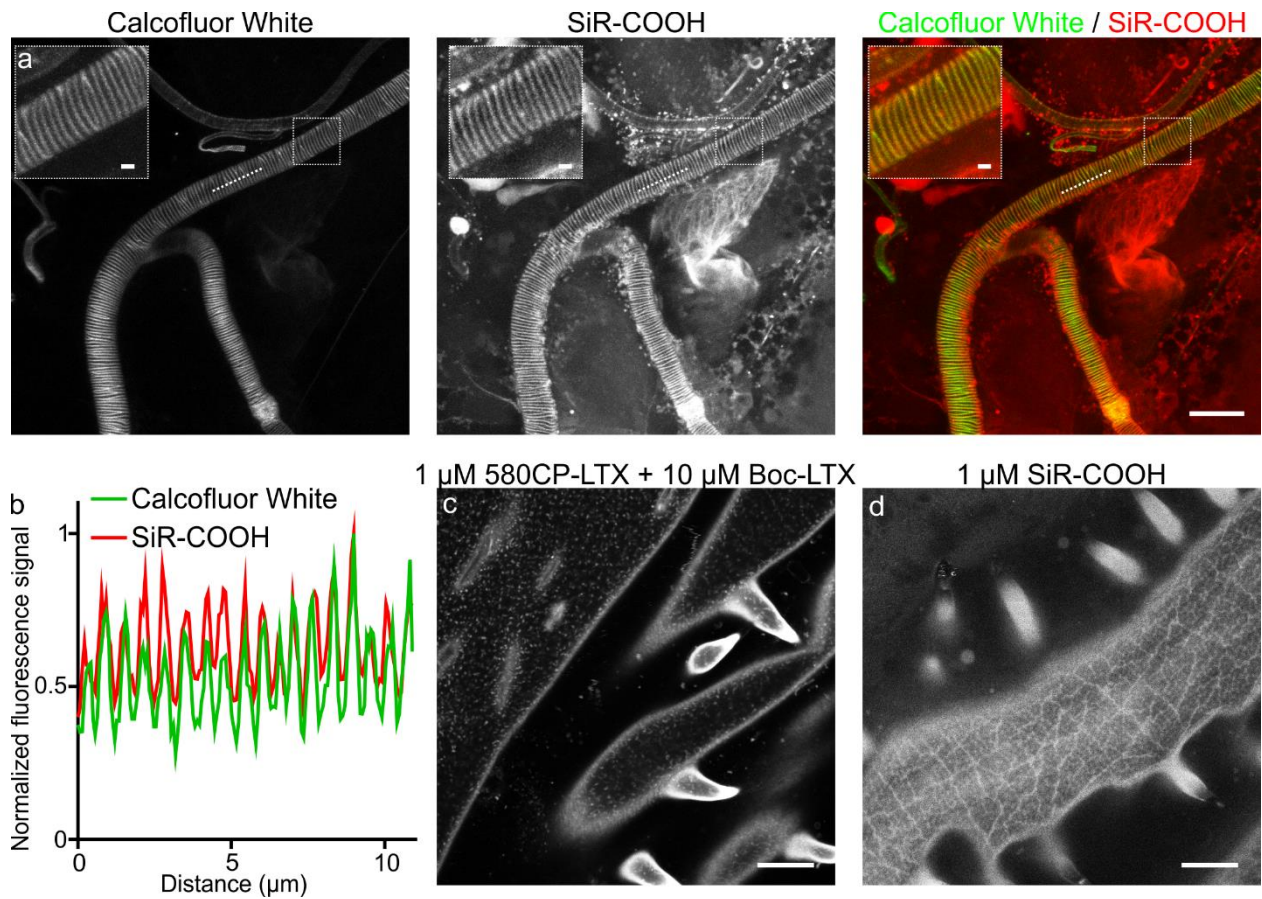


Figure S16. Confocal images of *Drosophila melanogaster* larvae tracheoles and cuticle. (a) Co-staining of tracheoles with 1 μM chitin-specific dye Calcofluor White M2R and 1 μM SiR-COOH. White rectangle indicates zoom-in area that is shown in the insert. (b) Fluorescence intensity profiles of Calcofluor White M2R and SiR-COOH taken along dashed line shown in (a) panels. Staining of cuticle with (c) a mixture of 1 μM 580CP-LTX and 10 μM non-fluorescent Boc-LTX, or (d) 1 μM SiR-COOH. Dissected *D. melanogaster* larvae were incubated with indicated probes or mixtures in PBS for 1 h at room temperature. Tissues were washed two times with PBS and imaged on a Leica SP8 (a, b) and Abberior STED 775 QUAD scanning microscope (c). Scale bar in the large field of view: 10 μm , insert: 1 μm .

Video S1. Confocal time series of microtubule dynamics in living human primary dermal fibroblasts stained with 62.5 nM 510R-CTX probe. Living cells were incubated with probe for 1 h at 37°C and washed once with HBSS before imaging in growth DMEM media at room temperature. Time lapse was acquired on a 587nm STED microscope with turned off depletion laser.

Video S2. Confocal time series of microtubule dynamics in living human primary dermal fibroblasts stained with 62.5 nM 580CP-LTX probe. Living cells were incubated with probe for 1 h at 37°C and washed once with HBSS before imaging in growth DMEM media at room temperature. Time lapse was acquired on an Abberior STED 775 QUAD scanning microscope.

Video S3. Confocal time series of microtubule dynamics in living human primary dermal fibroblasts stained with 250 nM GeR-DTX probe. Living cells were incubated with probe for 1 h at 37°C and washed once with HBSS before imaging in growth DMEM media at room temperature. Time lapse was acquired on an Abberior STED 775 QUAD scanning microscope.

Video S4. Confocal time series of microtubule dynamics in living human primary dermal fibroblasts stained with 62.5 nM SiR-CTX probe. Living cells were incubated with probe for 1 h at 37°C and washed once with HBSS before imaging in growth DMEM media at room temperature. Time lapse was acquired on an Abberior STED 775 QUAD scanning microscope.

Video S5. Confocal time series of microtubule dynamics in *Drosophila melanogaster* larvae living muscle tissue stained with 1 μM SiR-CTX probe. The muscle tissue was incubated with probe for 1 h at room temperature and washed once with PBS before imaging. Time lapse was acquired on an Abberior STED 775 QUAD scanning microscope.

Supplementary Tables

Table S1. Photophysical properties of fluorescent dyes used in this study.

Probe	Absorbance max. (nm)	Fluorescence max. (nm)	QY in PBS	QY in PBS with 0.1% SDS	Fluorescence lifetime (ns)	D _{0.5} [*]	Ref.
510R-COOH	496	520	0.90	0.92	3.8	52 ^{**}	3
580CP-COOH	582	607	0.62	0.63	3.6	35	4
GeR-COOH	634	655	0.43	0.47	2.7	65	5
SiR-COOH	645	661	0.41	0.46	2.7	65	6

Note: * D_{0.5} corresponds to the dielectric constant at which dye has half maximum absorbance. ** D_{0.5} for 510R-COOH is determined in this study.

Table S2. Photophysical properties of fluorescent tubulin probes.

Probe	Absorbance max. (nm)	Fluorescence max. (nm)	QY in PBS	QY in PBS with 0.1% SDS	cLogP [*]	
					Zwitterion	Spirolactone
510R-DTX			0.69	0.95	4.43	8.86
510R-CTX	502	526	0.62	0.94	5.79	10.22
510R-LTX			<0.1	0.94	5.67	10.09
580CP-DTX			0.48	0.65	3.84	7.39
580CP-CTX	588	610	0.48	0.62	5.20	8.74
580CP-LTX			0.20	0.65	5.07	8.62
GeR-DTX			0.44	0.58	1.85	10.59
GeR-CTX	640	660	0.25	0.60	3.21	11.95
GeR-LTX			<0.1	0.56	3.08	11.83
SiR-DTX			0.36	0.54	2.41	9.34
SiR-CTX	650	670	0.36	0.59	3.76	10.69
SiR-LTX			<0.1	0.55	3.64	10.57

Note: * Calculated with ChemDraw 15.1 (PerkinElmer).

Table S3. Properties of fluorescent tubulin probes.

Probe	Fl. Increase SDS/BSA (fold) [*]	Fl. Increase Tubulin/BSA (fold) [*]	Apparent polymerization rate ($\times 10^{-3} \text{ s}^{-1}$) ^{**}	Cytotoxicity threshold (nM)	Apparent microtubule FWHM (nm) ^{***}	I _{sat} (MW/cm ²) ^{**}
510R-DTX	3.9 ± 0.9	4.1 ± 0.5	6.1 ± 0.8	> 1000	-	-
510R-CTX	13 ± 1	11 ± 2	8.5 ± 1.0	≤ 62.5	36 ± 14	0.09 ± 0.01
510R-LTX	63 ± 10	1.6 ± 0.2	2.7 ± 0.1	> 1000	-	-
580CP-DTX	1.5 ± 0.3	1.5 ± 0.1	4.1 ± 0.4	> 1000	55 ± 21	4.3 ± 0.6
580CP-CTX	1.9 ± 0.4	1.6 ± 0.1	1.9 ± 0.3	≤ 62.5	57 ± 16	4.1 ± 0.5
580CP-LTX	5.0 ± 0.3	3.4 ± 0.3	1.5 ± 0.2	≤ 250	59 ± 18	4.9 ± 0.6
GeR-DTX	24 ± 2	6.3 ± 2.7	2.5 ± 0.4	≤ 250	41 ± 17	2.5 ± 0.3
GeR-CTX	47 ± 4	32 ± 5	2.8 ± 0.1	<< 62.5	42 ± 14	0.9 ± 0.1
GeR-LTX	262 ± 24	18 ± 3	2.3 ± 0.1	<< 62.5	-	-
SiR-DTX	16 ± 3	7 ± 3	4.2 ± 0.1	≤ 250	39 ± 10 ^{****}	-
SiR-CTX	44 ± 2	9 ± 4	2.3 ± 0.4	≤ 62.5	35 ± 13	1.0 ± 0.1
SiR-LTX	356 ± 24	2.8 ± 0.6	2.5 ± 0.1	> 1000	-	-

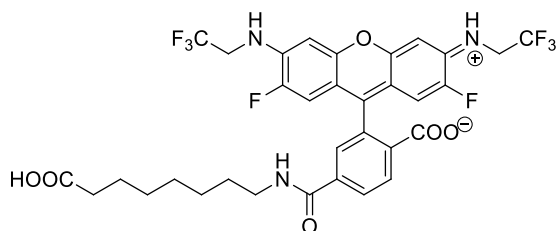
Note: * Data presented as mean value ± standard deviation. ** Data presented as fitted mean value ± standard error of the mean. *** Minimal FWHM values obtained from STED images. Data presented as mean value ± standard deviation **** Data from ref. ⁷.

Supplementary methods

General materials and methods: Flash chromatography was performed on Merck Silica gel 60, 0.04–0.063 mm (Cat. No. 815360) or using Biotage Isolera flash purification system with a cartridge and solvent gradient indicated. Reverse-phase chromatography was run on Polygoprep 60–50 C18 from Macheray-Nagel (Düren, Germany; Cat. No. 711500). NMR spectra were recorded at ambient temperature with Agilent 400-MR spectrometer (MPI-BPC Göttingen) at 400.06 MHz (^1H) and 100.60 MHz (^{13}C) and are reported in ppm. All ^1H spectra are referenced to tetramethylsilane ($\delta = 0$ ppm) using the signals of the residual protons of CHCl_3 (7.26 ppm) in CDCl_3 , acetone- d_5 (2.05 ppm) in acetone- d_6 , CHD_2OD (3.31 ppm) in CD_3OD or DMSO- d_5 (2.50 ppm) in DMSO- d_6 . ^{13}C spectra are referenced to tetramethylsilane ($\delta = 0$ ppm) using the signals of the solvent: CDCl_3 (77.16 ppm), acetone- d_6 (CD_3 , 29.84 ppm), CD_3OD (49.00 ppm) or DMSO- d_6 (39.52 ppm). Multiplicities of signals are described as follows: s = singlet, d = doublet, t = triplet, q = quartet, m = multiplet or overlap of signals; br. s = broad signal. Coupling constants (J) are given in Hz. For the ^{13}C chemical shifts obtained by indirect detection from HSQC experiments (resolution in F1: $t_1 = 256$), only H-coupled C-nuclei are resolved. Low-resolution mass spectra (50 – 3500 m/z) with electro-spray ionization (ESI) were recorded on a Varian 500-MS spectrometer (Agilent) at MPI-BPC Göttingen. High-resolution mass spectra (ESI-HRMS) were recorded on a MICROTOF spectrometer (Bruker) equipped with ESI ion source (Apollo) and direct injector with LC autosampler Agilent RR 1200 (Georg-August-Universität Göttingen). Liquid chromatography (HPLC) was performed using Knauer Smartline liquid chromatography system: two pumps (1000), UV-detector 2500, the column thermostat 4000, the mixing chamber and the injection valve with 20 μL and 100 μL loops for the analytical and preparative columns, respectively; 6-port-3-channel switching valve. Analytical column: Eurospher 100 C18, 10 μm , 150 \times 4 mm, solvent A: acetonitrile + 0.1% v/v TFA, solvent B: H_2O + 0.1% v/v TFA; temperature 20 $^\circ\text{C}$. Preparative column: Kinetex 100 C18, 5 μm , 250 \times 21 mm solvent A: acetonitrile, solvent B: H_2O + 0.05% v/v TFA; temperature 20 $^\circ\text{C}$; Analytical TLC was performed on Merck ready-to-use plates with silica gel 60 (F₂₅₄).

Chemical synthesis

510R-C8-COOH



510R³ (8 mg, 14 μmol) was dissolved in dry DMSO (0.5 ml). DIEA (15 μl , 86 μmol) and TSTU (5.6 mg, 19 μmol) were added and stirred for 5 min at r.t. Then 8-aminooctanoic acid (8.5 mg, 53 μmol) was added and the suspension was sonicated for 1 h at r.t. (conversion to *N*-hydroxysuccinimidyl ester can be controlled by HPLC). Then H_2O was added (200 μl), and the reaction mixture was stirred at room temperature for 20 min. The title compound was isolated by flash column chromatography on reversed phase (Interchim PuriFlash PF-30C₁₈HC-F0012 20g, 80 \times 16 mm; gradient 0% to 100% MeCN in H_2O + 0.1% HCOOH). The fractions containing the product were lyophilized. Yield – 7 mg (70%) of orange solid. HPLC: $t_{\text{R}} = 7.9$ min (A/B: 30/70 – 100/0 in 15 min, 1.2 ml/min, 500 nm).

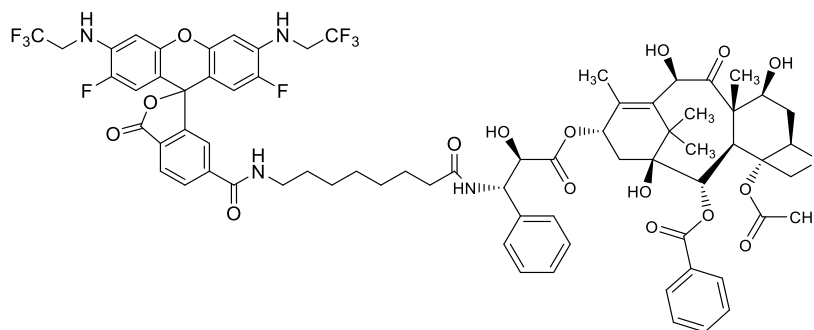
^1H NMR (400 MHz, $\text{DMSO-}d_6$): δ = 8.65 (t, J = 5.6, 1H, NH), 8.13 (dd, J = 8.0, 1.4, 1H, H-5'), 8.03 (d, J = 8.1, 1H, H-4'), 7.66 – 7.60 (m, 1H, H-7'), 6.83 (d, J = 7.6, 2H, H-4/5), 6.67 (q, J = 6.1, 2H, NH), 6.41 (d, J = 11.8, 2H, H-2/7), 4.04 (dd, J = 11.6, 6.2, 4H, $2 \times \text{CH}_2\text{CF}_3$), 3.16 (q, J = 7.4, 6.8, 2H, CH_2NH), 2.11 (t, J = 7.3, 2H, CH_2COOH), 1.41 (m, J = 6.8, 6.1, 4H, $2 \times \text{CH}_2$), 1.20 (m, 4H, $2 \times \text{CH}_2$).

^{13}C NMR (101 MHz, $\text{DMSO-}d_6$): δ = 168.3 (CO), 165.1 (CO), 152.0 (CO), 148.7, 148.5, 146.3, 141.2, 138.8, 130.0, 128.6, 125.9 (q, $^1J_{\text{CF}} = 281$, CF_3), 125.6, 122.4, 112.9 (d, $^2J_{\text{CF}} = 20$, C-1/8), 105.2, 99.4, 83.9, 66.7, 46.0, 43.7 (d, $^2J_{\text{CF}} = 32$, CH_2CF_3), 29.1, 28.8, 28.7, 26.6, 24.9.

ESI-MS, positive mode: m/z (rel. int., %) = 716 (100) $[\text{M}+\text{H}]^+$.

HRMS (m/z): $[\text{M}+\text{H}]^+$ calcd. for $\text{C}_{33}\text{H}_{29}\text{F}_8\text{N}_3\text{O}_6$, 716.2001; found, 716.1981.

510R-DTX



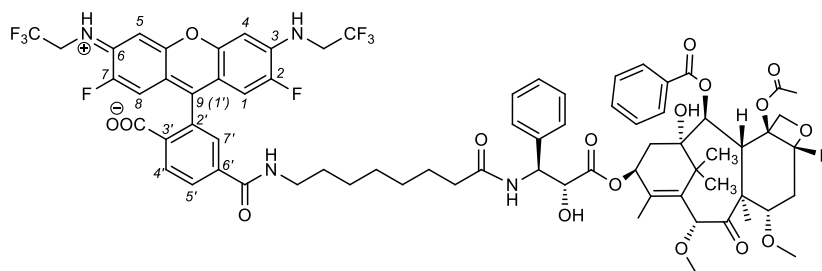
Docetaxel (Carbosynth, Cat. No. FD10817) with N-Boc protecting group (10 mg, 12 μmol) was dissolved in formic acid (0.4 ml) and incubated at r.t. for 30 min according to procedure described in ref⁷. Then the solvent was evaporated under reduced pressure and the residue was dried under high vacuum for 2 h. The crude 3'-aminodocetaxel formate was used in the next step without further purification.

510R-C8-COOH (67 μl of a 35.0 mM solution in DMSO, 2.3 μmol) was treated under argon atmosphere with DIEA (4.6 mg, 35.3 μmol) and TSTU (75 μl of a 55 mM DMSO, 14 μmol). After 5 min, 3'-aminodocetaxel (3.2 mg, 4.5 μmol) was added and incubated overnight at r.t. The product was purified by flash column chromatography (Interchim PuriFlash PF-30C₁₈HC-F0012 20g, 80 \times 16 mm; gradient 0% to 100% MeCN in H₂O + 0.1% HCOOH). The fractions containing the product were lyophilized. Yield – 1.0 mg (30%) of orange solid. HPLC: t_R = 8.3 min (A/B: 30/70 – 100/0 in 15 min, 1.2 ml/min, 500 nm).

ESI-MS, positive mode: m/z (rel. int., %) = 1405 (100) $[\text{M}+\text{H}]^+$.

HRMS (m/z): $[\text{M}+\text{H}]^+$ calcd. for $\text{C}_{71}\text{H}_{72}\text{F}_8\text{N}_4\text{O}_{17}$, 1405.4837; found, 1405.4811.

510R-CTX



Cabazitaxel (Carbosynth, Cat. No. FC19621) with N-Boc protecting group (10 mg, 12 μmol) was dissolved in formic acid (0.4 ml) and incubated at r.t. for 30 min according to procedure described in ref⁷. Then the solvent was evaporated under reduced pressure and the residue was dried under high vacuum for 2 h. The crude 3'-aminocabazitaxel formate was used for the next step without further purification.

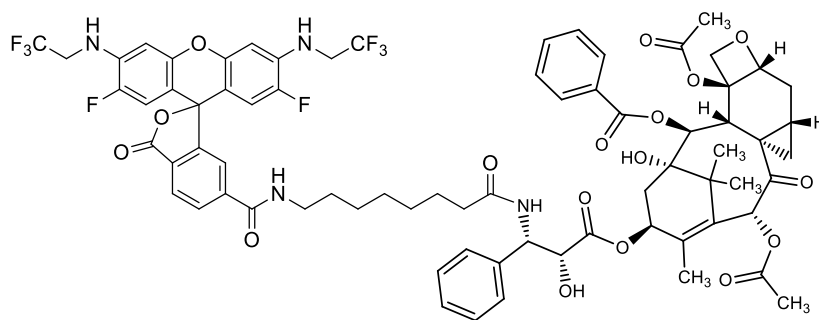
510R-CTX was prepared from 510R-C8-COOH (67 μl of a 35.0 mM solution in dry DMSO, 2.3 μmol) 3'-aminocabazitaxel (3.1 mg, 4.2 μmol), DIEA (4.6 mg, 35 μmol) and TSTU (75 μl of a 55 mM DMSO, 13.8 μmol) according to the method described above for the **510R-DTX**. The product was purified by flash column chromatography (Interchim PuriFlash PF-30C₁₈HC-F0012 20g, 80 \times 16 mm; gradient 0% to 100% MeCN in H₂O + 0.1% HCOOH). The fractions containing the product were lyophilized. Yield – 1.0 mg (30%) of orange solid. HPLC: t_{R} = 9.0 min (A/B: 30/70 – 100/0 in 15 min, 1.2 ml/min, 500 nm).

¹H NMR (600 MHz, DMSO-*d*₆): δ = 8.63 (t, J = 5.6, 1H, CONH), 8.36 (d, J = 9.1, 1H, CONH), 8.15 (dd, J = 8.0, 1.4, 1H, H-5'), 8.05 (d, J = 8.0, 1H, H-4'), 7.96 (dd, J = 7.0, 1.3, 2H, Bz), 7.69 – 7.65 (m, 2H, H-7', Bz), 7.58 (t, J = 7.6, 2H, Bz), 7.36 – 7.32 (m, 2H, Ph), 7.30 – 7.28 (m, 2H, Ph), 7.17 (t, J = 7.3, 1H, Ph), 6.89 (d, J = 7.3, 2H, H-4/5), 6.46 (d, J = 11.6, 2H, H-2/7), 5.95 – 5.90 (m, 1H, CH₂CHO), 5.37 (d, J = 7.2, 1H, CH), 5.24 (dd, J = 9.1, 5.9, 1H, CH-Ph), 4.94 (m, 1H, CH(OH)CO₂), 4.69 (s, 1H, CH), 4.40 (d, J = 6.7, 1H, CHOH), 4.14 – 3.99 (m, 6H, CH₂, CH₂CF₃), 3.74 – 3.77 (m, 1H, MeOCH), 3.46 – 3.45 (m, 1H, CH), 3.39 – 3.38 (m, 2H, CH₂NH), 3.28 (s, 3H, OMe), 3.19 (s, 3H, OMe), 3.18 – 3.13 (m, 2H, CH₂), 2.67 – 2.60 (m, 1H, CH₂), 2.23 (s, 3H, Me, OAc), 2.16 – 2.11 (m, 1H, CH), 1.98 – 1.91 (m, 1H, CH₂CHO), 1.86 – 1.79 (m, 4H, Me-C=, CH₂CHO), 1.52 – 1.48 (m, 4H, CH₂, Me), 1.46 – 1.38 (m, 4H, CH₂, 2 \times CH₂ linker), 1.26 – 1.15 (m, 6H, 3 \times CH₂ linker), 1.01 (s, 3H, Me), 0.95 (s, 3H, Me).

ESI-MS, positive mode: m/z (rel. int., %) = 1433 (100) [M+H]⁺.

HRMS (m/z): [M+H]⁺ calcd. for C₇₃H₇₆F₈N₄O₁₇, 1433.5150; found, 1433.5125.

510R-LTX



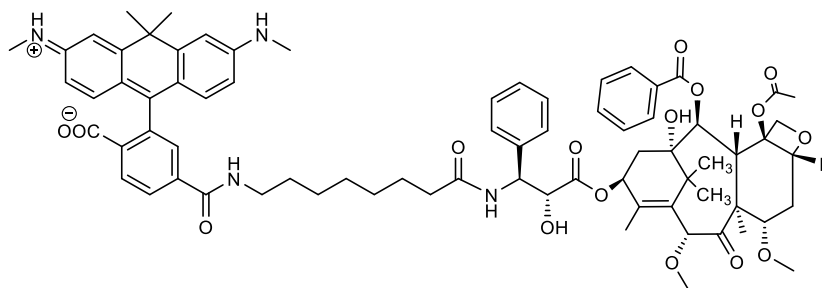
Boc protected Larotaxel (Toronto research Chemicals, Cat. No. L176000, 18 mg, 23 μmol) was dissolved in formic acid (0.6 ml) and incubated at room temperature for 30 min according to procedure described in ref⁷. Then the solvent was evaporated under reduced pressure and the residue was dried under high vacuum for 2 h. The crude 3'-aminolarotaxel formate was used for the next step without further purification.

510R-LTX was prepared from 510R-C8-COOH (67 μl of a 35.0 mM solution in DMSO, 2.3 μmol), 3'-aminolarotaxel (7 mg, 9.6 μmol), DIEA (4.6 mg, 35.3 μmol) and TSTU (75 μl of a 55 mM DMSO, 13.8 μmol) according to the method described above for the **510R-DTX**. The product was purified by flash column chromatography (Interchim PuriFlash PF-30C₁₈HC-F0012 20g, 80 \times 16 mm; gradient 0% to 100% MeCN in H₂O + 0.1% HCOOH). The fractions containing the product were lyophilized. Yield – 1.2 mg (37%) of orange solid. HPLC: t_R = 9.2 min (A/B: 30/70 – 100/0 in 15 min, 1.2 ml/min, 500 nm).

ESI-MS, positive mode: m/z (rel. int., %) = 1429 (100) [M+H]⁺.

HRMS (m/z): [M+H]⁺ calcd. for C₇₃H₇₂F₈N₄O₁₇, 1429.4837; found, 1429.4815.

580CP-CTX

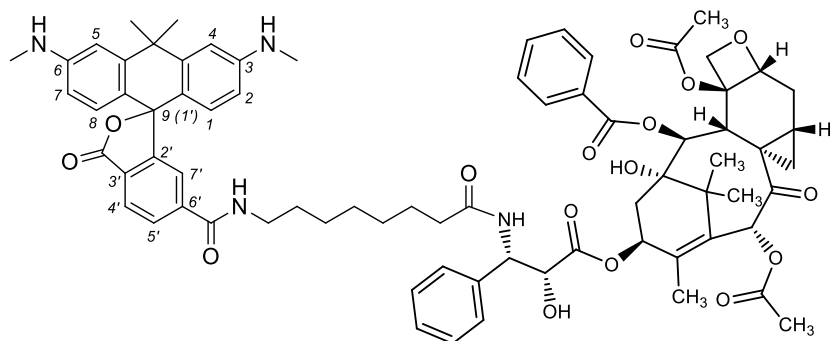


580CP-CTX was prepared from 580CP-C8-COOH⁸ (0.75 mg, 1.3 μmol) 3'-aminocabazitaxel (2.0 mg, 2.7 μmol), DIEA (1.4 mg, 10.6 μmol) and TSTU (75 μl of a 55 mM DMSO, 13.8 μmol) according to the method described above for **510R-DTX**. The product was purified by preparative HPLC and lyophilized. Yield – 1.2 mg (69%) of purple solid. HPLC: t_R = 11.5 min (A/B: 20/80 – 50/50 in 15 min, 1.2 ml/min, 600 nm).

ESI-MS, positive mode: m/z (rel. int., %) = 1288 (100) [M+H]⁺.

HRMS (m/z): [M+H]⁺ calcd. for C₇₄H₈₆N₄O₁₆, 1287.6112; found, 1287.6114.

580CP-LTX



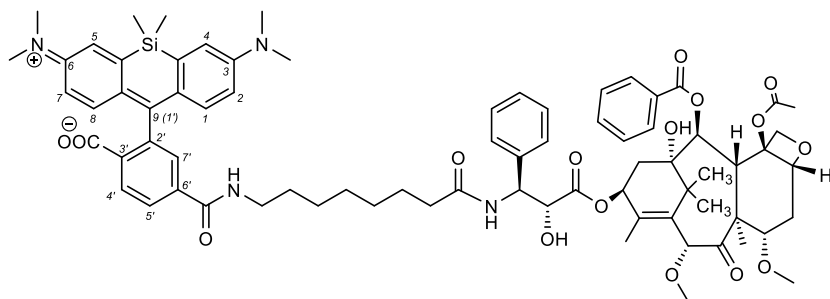
580CP-LTX was prepared from 580CP-C8-COOH⁸ (1.5 mg, 2.6 μmol) 3'-aminolarotaxel (4.0 mg, 5.5 μmol), DIEA (2.7 mg, 21.2 μmol) and TSTU (5.9 mg, 19.6 μmol) according to the method described above for **510R-DTX**. The product was purified by preparative HPLC and lyophilized. Yield –2.0 mg (61%) of purple solid. HPLC: t_{R} = 6.3 min (A/B: 20/80 – 100/0 in 10 min, 1.2 ml/min, 600 nm).

¹H NMR (400 MHz, DMSO-*d*₆) δ = 8.69 (t, J = 5.7, 1H, CONH), 8.33 (d, J = 9.2, 1H, CONH), 8.22 – 8.13 (m, 2H, H-4', H-5'), 8.05 – 7.99 (m, 2H, Bz), 7.77 – 7.70 (m, 1H, H-7'), 7.63 (m, 1H, Bz), 7.61 – 7.56 (m, 2H, Bz), 7.39 – 7.26 (m, 4H, Ph), 7.22 – 7.12 (m, 1H, Ph), 7.10 (br. s, 2H, H-4/5), 6.78 (br. s, 2H, H-1/8), 6.62 (d, J = 8.0, 2H, H-2/7), 6.12 (s, 1H, CH), 5.95 (t, J = 9.0, 1H, CH), 5.43 (d, J = 7.6, 1H, CH), 5.33 (dd, J = 9.2, 5.2, 1H, CH-Ph), 4.78 – 4.67 (m, 2H, **CH(OH)CO₂**, OH), 4.49 (d, J = 5.2, 1H, **CHOH**), 4.06 – 3.94 (m, 2H, CH₂), 3.90 (d, J = 7.6, 1H, CH), 3.26 – 3.15 (m, 2H, **CH₂NH**), 2.97 (br. s, 6H, N(Me)₂), 2.30 (s, 4H, CH₂, Me, OAc), 2.12 (s, 4H, CH₂, Me, OAc), 2.08 – 1.97 (m, 1H, CH₂), 1.97 – 1.85 (m, 1H, CH₂), 1.75 (s, 3H, Me-C=), 1.74 (m, 3H, Me), 1.64 (s, 3H, Me), 1.56 – 1.51 (m, 1H, CH₂), 1.49 – 1.39 (m, 5H, CH₂), 1.26 – 1.14 (m, 9H, CH, CH₂), 1.11 (s, 3H, Me), 1.07 (s, 3H, Me).

ESI-MS, positive mode: m/z (rel. int., %) = 1284 (100) [M+H]⁺.

HRMS (m/z): [M+H]⁺ calcd. for C₇₄H₈₂N₄O₁₆, 1283.5799; found, 1283.5801

SiR-CTX



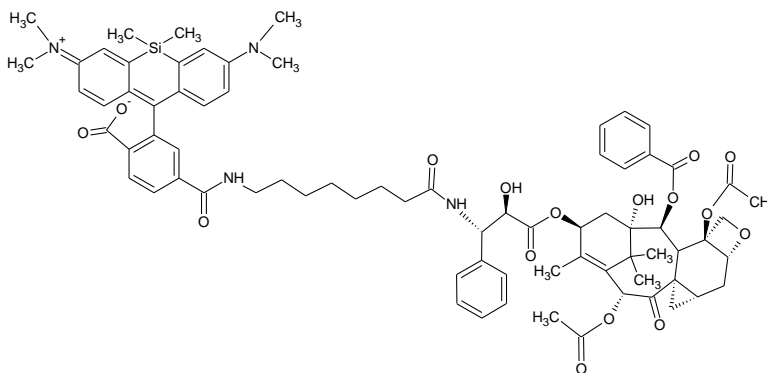
SiR-CTX was prepared from SiR⁷ (1.5 mg, 2.4 μmol) 3'-aminocabazitaxel (3.8 mg, 5.2 μmol), DIEA (2.7 mg, 21.2 μmol) and TSTU (5.5 mg, 18.2 μmol) according to the method described above for **510R-DTX**. The product was purified by preparative HPLC and lyophilized. Yield –1.4 mg (44%) of blue solid. HPLC: t_{R} = 10.6 min (A/B: 30/70 – 100/0 in 15 min, 1.2 ml/min, 630 nm).

^1H NMR (400 MHz, $\text{DMSO-}d_6$) δ = 8.69 (t, J = 5.6, 1H, CONH), 8.34 (d, J = 9.1, 1H, CONH), 8.06 (dd, J = 8.1, 1.4, 1H, H-5'), 8.01 (d, J = 8.1, 1H, H-4'), 7.99 – 7.95 (m, 2H, Bz), 7.70 – 7.63 (m, 2H, H-7', Bz), 7.61 – 7.55 (m, 2H, Bz), 7.38 – 7.28 (m, 5H, H-Ph), 7.02 (s, 2H, H-4/5), 6.67 – 6.60 (m, 4H, H-1/2/7/8), 6.00 – 5.87 (m, 1H, CH_2CHO), 5.42 – 5.35 (m, 1H, CH), 5.28 (dd, J = 9.1, 5.7, 1H, CH-Ph), 4.95 (dd, J = 9.6, 2.0, 1H, CH), 4.72 – 4.65 (m, 1H, $\text{CH}(\text{OH})\text{CO}_2$), 4.64 (br.s, 1H, OH), 4.40 (d, J = 5.7, 1H, CHOH), 4.02 (s, 2H, CH_2), 3.75 – 3.74 (m, 1H, MeOCH), 3.67 – 3.58 (m, 1H, CH), 3.32 – 3.28 (m, 5H, CH_2NH , OMe), 3.23 – 3.13 (m, 5H, CH_2 , OMe), 2.92 (s, 12H, $2 \times \text{N}(\text{Me})_2$), 2.70 – 2.54 (m, 1H, CH_2), 2.28 – 2.19 (m, 3H, Me, OAc), 2.18 – 2.10 (m, 1H, CH), 2.01 – 1.92 (m, 1H, CH_2CHO), 1.85 – 1.78 (m, 4H, Me, CH_2CHO), 1.55 – 1.48 (m, 4H, CH_2 , Me-C=), 1.53 – 1.38 (m, 4H, $2 \times \text{CH}_2$ linker), 1.27 – 1.12 (m, 6H, CH_2 , $3 \times \text{CH}_2$ linker), 1.08 – 0.99 (m, 3H, $\frac{1}{2} \times \text{C}(\text{Me})_2$), 0.99 – 0.95 (m, 3H, $\frac{1}{2} \times \text{C}(\text{Me})_2$), 0.63 (s, 3H, $\frac{1}{2} \times \text{Si}(\text{Me})_2$), 0.52 (s, 3H, $\frac{1}{2} \times \text{Si}(\text{Me})_2$).

ESI-MS, positive mode: m/z (rel. int., %) = 1332 (100) $[\text{M}+\text{H}]^+$.

HRMS (m/z): $[\text{M}+\text{H}]^+$ calcd. for $\text{C}_{75}\text{H}_{90}\text{N}_4\text{O}_{16}\text{Si}$, 1331.6194; found, 1331.6212.

SiR-LTX

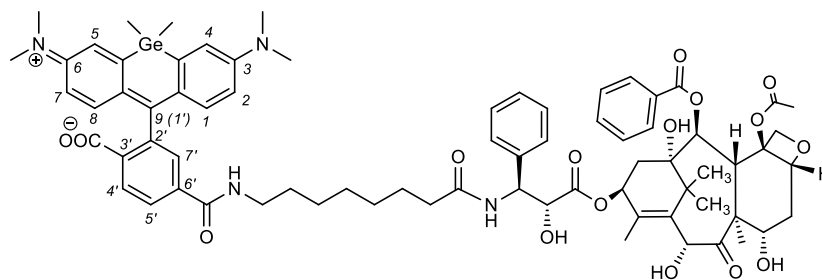


SiR-LTX was prepared from SiR⁷ (1.5 mg, 2.4 μmol) 3'-aminolarotaxel (3.8 mg, 5.2 μmol), DIEA (4.1 mg, 31.7 μmol) and TSTU (5.5 mg, 18.2 μmol) according to the method described above for **510R-DTX**. The product was purified by preparative HPLC and lyophilized. Yield –1.4 mg (44%) of blue solid. HPLC: t_{R} = 11.0 min (A/B: 30/70 – 100/0 in 15 min, 1.2 ml/min, 630 nm).

ESI-MS, positive mode: m/z (rel. int., %) = 1328 (100) $[\text{M}+\text{H}]^+$.

HRMS (m/z): $[\text{M}+\text{H}]^+$ calcd. for $\text{C}_{75}\text{H}_{86}\text{N}_4\text{O}_{16}\text{Si}$, 1327.5881; found, 1327.5914.

GeR-DTX



GeR-DTX was prepared from the GeR dye according to the literature procedure.⁵

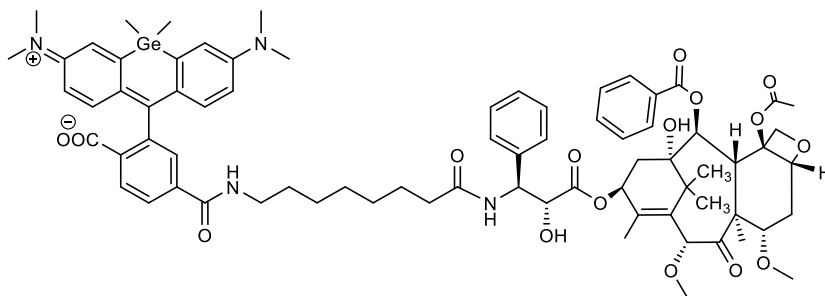
^1H NMR (400 MHz, acetone- d_6) δ = 8.16 – 8.11 (m, 3H, H-4', Bz), 8.06 (t, J = 5.7, 1H, CONH), 7.99 – 7.95 (m, 2H, H-5', H-7'), 7.67 – 7.61 (m, 1H, Bz), 7.61 – 7.52 (m, 3H, CONH, Bz), 7.49 – 7.44 (m, 2H, H-Ph), 7.40 – 7.34 (m, 2H, H-Ph), 7.29 – 7.22 (m, 1H, H-Ph), 7.09 (d, J = 2.9, 2H, H-4, H-5), 6.80 (d, J = 8.9, 2H, H-1, H-8), 6.56 (ddd, J = 8.9, 2.9, 1.3, 2H, H-2, H-7), 6.20 (t, J = 9.0, 1H, CHO–C=), 5.68 (d, J = 7.1, 1H, CHOBz), 5.60 (dd, J = 9.2, 3.6, 1H, CH(Ph)NH), 5.23 (s, 1H, CHOH–C=O), 4.94 (dd, J = 9.8, 2.0, 1H, CH–O), 4.71 (d, J = 3.7, 1H, CH(OH)CO₂), 4.31 (dd, J = 11.1, 6.5, 1H, CHOH), 4.21 – 4.10 (m, 2H, CH₂O), 3.94 (d, J = 7.6, 1H, CH), 3.81 (br.s, 1H, OH), 3.37 (q, J = 6.7, 2H, CH₂NH), 2.96 (s, 12H, 4 × Me, N(Me)₂), 2.50 – 2.35 (m, 2H, 2 × CH₂), 2.42 (s, 3H, Me, OAc), 2.31 – 2.17 (m, 3H, 2 × CH₂), 1.90 (d, J = 1.5, 3H, Me–C=), 1.83 (ddd, J = 14.0, 11.1, 2.3, 1H, CH₂), 1.72 (s, 3H, Me), 1.62 – 1.50 (m, 4H, 2 × CH₂ linker), 1.36 – 1.24 (m, 6H, 3 × CH₂ linker), 1.21 (s, 3H, ½ × C(Me)₂), 1.15 (s, 3H, ½ × C(Me)₂), 0.81 (s, 3H, ½ × Ge(Me)₂), 0.72 (s, 3H, ½ × Ge(Me)₂).

^{13}C NMR (101 MHz, acetone- d_6) δ 133.8 (CH), 130.7 (CH), 129.2 (CH), 128.9 (CH), 128.7 (CH), 128.1 (CH), 127.95 (CH), 127.92 (CH), 126.2 (CH), 124.6 (CH), 117.8 (CH), 113.1 (CH), 84.9 (CH), 76.7 (CH₂), 75.8 (CH), 74.9 (CH), 74.5 (CH), 72.1 (CH), 71.9 (CH), 55.6 (CH), 47.2 (CH), 40.3 (CH₂), 40.1 (Me), 37.4 (CH₂, ×2.45 ppm, ×1.84 ppm), 36.7 (CH₂, ×2.37 ppm, ×2.22 ppm), 36.3 (CH₂), 30.0 (CH₂), 36.7 (CH₂), 29.6 (CH₂), 27.3 (CH₂), 26.9 (Me), 26.2 (CH₂), 22.8 (Me), 21.2 (Me), 14.2 (Me), 10.2 (Me), 0.3 (Me), -2.5 (Me).

ESI-MS, positive mode: m/z (rel. int., %) = 1371.5 [M+Na]⁺.

HRMS (m/z): [M+Na]⁺ calcd. for C₇₃H₈₆N₄O₁₆Ge, 1371.5165; found, 1371.5111.

GeR-CTX

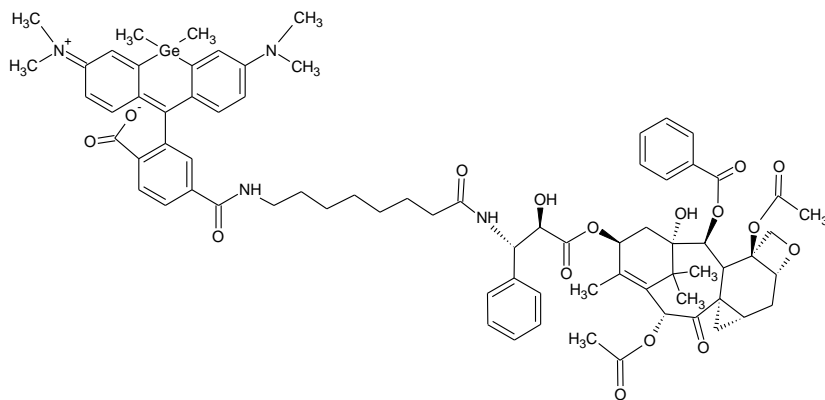


Cabazitaxel-GeR was prepared from GeR⁵ (1.3 mg, 2.0 μmol) 3'-aminocabazitaxel (4.4 mg, 6.0 μmol), DIEA (2.7 mg, 21.2 μmol) and TSTU (5.5 mg, 18.2 μmol) according to the method described above for the **510R-DTX**. The product was purified by preparative HPLC and lyophilized. Yield –0.5 mg (18%) of blue solid. HPLC: t_R = 10.6 min (A/B: 30/70 – 100/0 in 15 min, 1.2 ml/min, 630 nm).

ESI-MS, positive mode: m/z (rel. int., %) = 1378 (100) [M+H]⁺.

HRMS (m/z): [M+H]⁺ calcd. for C₇₅H₉₀GeN₄O₁₆, 1377.5659; found, 1377.5688.

GeR-LTX



GeR-LTX was prepared from SiR⁵ (1.3 mg, 2.0 μ mol) 3'-aminolarotaxel (2.9 mg, 3.9 μ mol), DIEA (2.7 mg, 21.2 μ mol) and TSTU (4.3 mg, 14.3 μ mol) according to the method described above for the **510R-DTX**. The product was purified by preparative HPLC and lyophilized. Yield – 0.5 mg (18%) of blue solid. HPLC: t_R = 10.9 min (A/B: 30/70 – 100/0 in 15 min, 1.2 ml/min, 630 nm).

ESI-MS, positive mode: m/z (rel. int., %) = 1374 (100) $[M+H]^+$.

HRMS (m/z): $[M+H]^+$ calcd. for C₇₅H₈₆GeN₄O₁₆, 1373.5323; found, 1373.5355.

Supplementary references

1. E. H. Kellogg, N. M. A. Hejab, S. Howes, P. Northcote, J. H. Miller, J. F. Diaz, K. H. Downing and E. Nogales, *J. Mol. Biol.*, 2017, **429**, 633-646.
2. G. Åkerlöf and A. O. Short, *J. Am. Chem. Soc.*, 1936, **58**, 1241–1243.
3. G. Y. Mitronova, V. N. Belov, M. L. Bossi, C. A. Wurm, L. Meyer, R. Medda, G. Moneron, S. Bretschneider, C. Eggeling, S. Jakobs and S. W. Hell, *Chemistry*, 2010, **16**, 4477-4488.
4. A. N. Butkevich, G. Y. Mitronova, S. C. Sidenstein, J. L. Klocke, D. Kamin, D. N. Meineke, E. D'Este, P. T. Kraemer, J. G. Danzl, V. N. Belov and S. W. Hell, *Angew. Chem. Int. Ed. Engl.*, 2016, **55**, 3290-3294.
5. A. N. Butkevich, V. N. Belov, K. Kolmakov, V. V. Sokolov, H. Shojaei, S. C. Sidenstein, D. Kamin, J. Matthias, R. Vlijm, J. Engelhardt and S. W. Hell, *Chemistry – A European Journal*, 2017, **23**, 12114-12119.
6. G. Lukinavičius, K. Umezawa, N. Olivier, A. Honigmann, G. Yang, T. Plass, V. Mueller, L. Reymond, I. R. Correa, Jr., Z. G. Luo, C. Schultz, E. A. Lemke, P. Heppenstall, C. Eggeling, S. Manley and K. Johnsson, *Nat. Chem.*, 2013, **5**, 132-139.
7. G. Lukinavičius, L. Reymond, E. D'Este, A. Masharina, F. Gottfert, H. Ta, A. Guther, M. Fournier, S. Rizzo, H. Waldmann, C. Blaukopf, C. Sommer, D. W. Gerlich, H. D. Arndt, S. W. Hell and K. Johnsson, *Nat. Methods*, 2014, **11**, 731-733.
8. F. R. Winter, M. Loidolt, V. Westphal, A. N. Butkevich, C. Gregor, S. J. Sahl and S. W. Hell, *Sci. Rep.*, 2017, **7**, 46492.